

**Tuning of Dielectric Parameters of CuTi-1223
Superconductor by Varying Chromium (Cr)
Nanoparticles contents**



by

Ahmed Saleh Raja
(302-FBAS/MSPHY/F14)

Supervisor

Dr. Muhammad Mumtaz

Assistant Professor

Department of Physics, FBAS,

IIU, Islamabad

Department of Physics

Faculty of Basic and Applied Sciences

International Islamic University, Islamabad, Pakistan,

(2017)



Accession No TH118282 ^{1/2/11}



MS
620.5
RAT

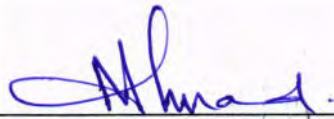
Nanotechnology
x-Rays diffraction
Nanomaterials.

Tuning of Dielectric Parameters of CuTi-1223 Superconductor by Varying Chromium (Cr) Nanoparticles contents

By

Ahmed Saleh Raja
(302-FBAS/MSPHY/F14)

This thesis submitted to Department of Physics, FBAS, International Islamic University
Islamabad for the award of degree of MS Physics



Chairman, Department of Physics
International Islamic University, Islamabad.



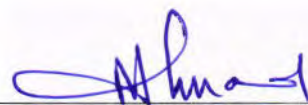
Dean, Faculty of Basic and Applied Sciences
International Islamic University, Islamabad.

Final Approval

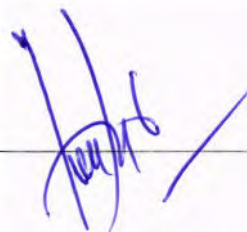
It is certified that the work presented in this thesis titled “**Tuning of Dielectric Parameters of CuTi-1223 Superconductor by Varying Chromium (Cr) Nanoparticles contents**” by **Ahmed Saleh Raja** (Reg. No.302-FBAS/MSPHY/F-14) fulfills the requirement for the award of degree of MS Physics from Department of Physics, International Islamic University Islamabad, Pakistan.

Viva Voice Committee

Chairman (Prof. Dr. Mushtaq Ahmed)
(Department of Physics)



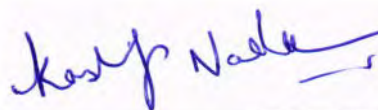
Supervisor (Dr. M. Mumtaz)



External Examiner (Prof. Dr. Ishaq Ahmed)



Internal Examiner (Dr. Kashif Nadeem)



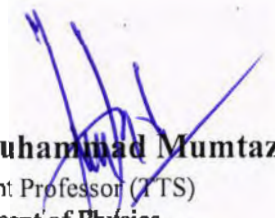
بِسْمِ اللَّهِ الرَّحْمَنِ الرَّحِيمِ

**DEDICATED
TO
MY BELOVED PARENTS
AND
RESPECTED TEACHERS**

Forwarding Sheet by Research Supervisor

The thesis titled "Tuning of Dielectric Parameters of CuTi-1223 Superconductor by Varying

Chromium (Cr) Nanoparticles contents" submitted by **Ahmed Saleh Raja**(Reg. No. 302-FBAS/MSPHY/F-14) in partial fulfillment of MS degree in Physics has been completed under my guidance and supervision. I am satisfied with the quality of his research work and allow him to submit this thesis for further process to graduate with Master of Science degree from Department of Physics, FBAS, as per International Islamic University Islamabad, Pakistan, rules and regulations.


Dr. Muhammad Mumtaz
Assistant Professor (TTS)
Department of Physics,
International Islamic University,
Islamabad.

Dated: 30-8-2017

Acknowledgement

I have no words to express my deepest sense of gratitude and numerous thanks to **Almighty Allah**, who enabled me to complete this study and with innumerable blessings for the **Holy Prophet Peace Be Upon Him** who is forever a torch of guidance and knowledge for the whole humanity.

I would like to thank my supervisor **Dr. Muhammad Mumtaz**. Firstly, for taking me on as a student and then for providing support, advice for letting me develop my own ideas, and for helping me make it to the end. I would like to pay lots of appreciation to all my teachers.

My journey wouldn't have been the same without the lab fellows for all the conversations that we had over the year, they always made me smile when the lab days just weren't going right. I appreciate the services of all my senior research colleagues **Liaqat Ali**, **M.Imran** and especially **Abrar Ahmed Khan** for being very supportive and co-operative all throughout my research work. I also pay special thanks to my lab fellow **Muhammad Navced** for being helpful in all my research work.

My humble and heartfelt gratitude is reserved for my beloved Parents and sister. Without their prayers and encouragement the completion of this task would have been a dream. I am extremely thankful to my brother **Shoaib Saleh Raja** for his sincere cooperation, sincere appreciation, motivation and considerate attitude throughout my tough time during the completion of this dissertation.

May Allah bless all these people.

Ahmed Saleh Raja

Table of Contents

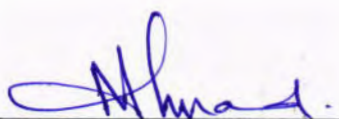
Chapter 1	1
Introduction	1
1.1 Historical background of superconductivity	1
1.2 Essential types of superconductivity	2
1.2.1 Zero electrical resistance	2
1.2.2 Perfect diamagnetism	2
1.3 Basic and important critical parameters of superconductors	3
1.3.1 Superconductor critical temperature.....	3
1.3.2 Critical magnetic field	4
1.3.3 Critical current.....	4
1.3.4 Critical current density	5
1.4 Relation between Critical temperature, magnetic field and current density	5
1.5 Types of superconductors.....	5
1.5.1 Type-I superconductors	5
1.5.2 Type II superconductors	6
1.6 High temerture superconductor	7
1.6.1 Tl-Ba-Ca-Cu-O superconductor	7
1.6.2 Hg-Ba-Ca-Cu-O superconductor	8
1.7 Experimental facts of superconductor.....	8
1.7.1 Jospheson junction effect.....	8
1.7.2 A.C.Jospheson junction effect	9
1.7.3 D.C.Jospheson junction effect	9
1.8 Meissner effect	9
1.9 Important theories of superconductivity	10
1.9.1 London theory.....	10
1.9.2 London penetration depth	11
1.10 BCS Theory	11
1.11 Introduction to dielectric materials	12
1.11.1 Dielectric polarization	13
1.12 Classification of polarization	14

Tuning of Dielectric Parameters of CuTl-1223 Superconductor by Varying Chromium (Cr) Nanoparticles contents

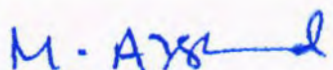
By

Ahmed Saleh Raja
(302-FBAS/MSPHY/F14)

This thesis submitted to Department of Physics, FBAS, International Islamic University
Islamabad for the award of degree of MS Physics



Chairman, Department of Physics
International Islamic University, Islamabad.



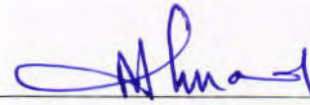
Dean, Faculty of Basic and Applied Sciences
International Islamic University, Islamabad.

Final Approval

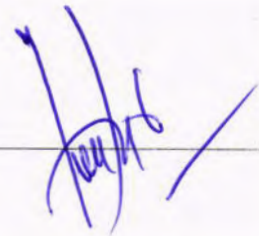
It is certified that the work presented in this thesis titled “**Tuning of Dielectric Parameters of CuTi-1223 Superconductor by Varying Chromium (Cr) Nanoparticles contents**” by **Ahmed Saleh Raja** (Reg. No.302-FBAS/MSPHY/F-14) fulfills the requirement for the award of degree of MS Physics from Department of Physics, International Islamic University Islamabad, Pakistan.

Viva Voice Committee

Chairman (Prof. Dr. Mushtaq Ahmed)
(Department of Physics)



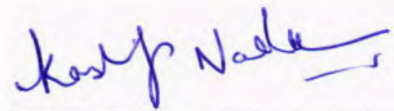
Supervisor (Dr. M. Mumtaz)



External Examiner (Prof. Dr. Ishaq Ahmed)



Internal Examiner (Dr. Kashif Nadeem)



بِسْمِ اللَّهِ الرَّحْمَنِ الرَّحِيمِ

**DEDICATED
TO
MY BELOVED PARENTS
AND
RESPECTED TEACHERS**

Declaration of Originality

I, **Ahmed Saleh Raja** Reg. No. 302-FBAS/MSPHY/F-14 student of MS Physics (Session 2014-2017), hereby declare that the work presented in the thesis titled **“Tuning of Dielectric Parameters of CuTi-1223 Superconductor by Varying Chromium (Cr) Nanoparticles contents”** in partial fulfillment of MS degree in Physics from International Islamic University Islamabad, Pakistan, is my own work and has not been published or submitted as research work or thesis in any form in any other university or institute in Pakistan or abroad.

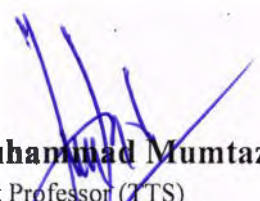


Ahmed Saleh Raja
(302-FBAS/MSPHY/F-14)

Dated: 30-8-2017

Forwarding Sheet by Research Supervisor

The thesis titled “**Tuning of Dielectric Parameters of CuTi-1223 Superconductor by Varying Chromium (Cr) Nanoparticles contents**” submitted by **Ahmed Saleh Raja**(Reg. No. 302-FBAS/MSPHY/F-14) in partial fulfillment of MS degree in Physics has been completed under my guidance and supervision. I am satisfied with the quality of his research work and allow him to submit this thesis for further process to graduate with Master of Science degree from Department of Physics, FBAS, as per International Islamic University Islamabad, Pakistan, rules and regulations.


Dr. Muhammad Mumtaz
Assistant Professor (TTS)
Department of Physics,
International Islamic University,
Islamabad.

Dated: 30-8-2017

Acknowledgement

I have no words to express my deepest sense of gratitude and numerous thanks to **Almighty Allah**, who enabled me to complete this study and with innumerable blessings for the **Holy Prophet Peace Be Upon Him** who is forever a torch of guidance and knowledge for the whole humanity.

I would like to thank my supervisor **Dr. Muhammad Mumtaz**. Firstly, for taking me on as a student and then for providing support, advice for letting me develop my own ideas, and for helping me make it to the end. I would like to pay lots of appreciation to all my teachers.

My journey wouldn't have been the same without the lab fellows for all the conversations that we had over the year, they always made me smile when the lab days just weren't going right. I appreciate the services of all my senior research colleagues **Liaqat Ali, M.Imran** and especially **Abrar Ahmed Khan** for being very supportive and co-operative all throughout my research work. I also pay special thanks to my lab fellow **Muhammad Naveed** for being helpful in all my research work.

My humble and heartfelt gratitude is reserved for my beloved Parents and sister. Without their prayers and encouragement the completion of this task would have been a dream. I am extremely thankful to my brother **Shoaib Saleh Raja** for his sincere cooperation, sincere appreciation, motivation and considerate attitude throughout my tough time during the completion of this dissertation.

May Allah bless all these people.

Ahmed Saleh Raja

Table of Contents

Chapter I	1
Introduction.....	1
1.1 Historical background of superconductivity	1
1.2 Essential types of superconductivity	2
1.2.1 Zero electrical resistance	2
1.2.2 Perfect diamagnetism	2
1.3 Basic and important critical parameters of superconductors	3
1.3.1 Superconductor critical temperature.....	3
1.3.2 Critical magnetic field	4
1.3.3 Critical current.....	4
1.3.4 Critical current density	5
1.4 Relation between Critical temperature, magnetic field and current density	5
1.5 Types of superconductors.....	5
1.5.1 Type-I superconductors	5
1.5.2 Type II superconductors	6
1.6 High temperature superconductor	7
1.6.1 Tl-Ba-Ca-Cu-O superconductor	7
1.6.2 Hg-Ba-Ca-Cu-O superconductor	8
1.7 Experimental facts of superconductor.....	8
1.7.1 Josephson junction effect.....	8
1.7.2 A.C.Josephson junction effect	9
1.7.3 D.C.Josephson junction effect	9
1.8 Meissner effect	9
1.9 Important theories of superconductivity	10
1.9.1 London theory.....	10
1.9.2 London penetration depth	11
1.10 BCS Theory	11
1.11 Introduction to dielectric materials	12
1.11.1 Dielectric polarization	13
1.12 Classification of polarization	14

1.12.1 Atomic polarization	14
1.12.2 Oriental (Dipolar polarization)	14
1.12.3 Ionic polarization	15
1.12.4 Interfacial polarization	15
1.13 Temperature dependent polarization	16
1.13.1 Frequency dependence of dielectric polarization	16
1.14 Classification of dielectric materials	16
1.14.1 Real part	16
1.14.2 Imaginary part	17
1.14.3 Tangent Loss ($\text{Tan}\delta$)	17
1.14.4 Ac conductivity	17
1.15 History of Nanotechnology	17
1.16 Nonmaterial's categories	17
1.16.1 Zero dimension (0-D) Nano materials	18
1.16.2 One dimension (1-D) Nano materials	18
1.16.3 Two dimension (2-D) Nano materials	18
1.16.4 Three dimension (3-D) Nano materials	18
Chapter 2	19
Literature review	22
Chapter 3	23
Synthesis and Characterization Techniques	23
3.1 Synthesis techniques	23
3.1.1 Solid State Reaction method	23
3.2 Sample preparation method	23
3.2.1 Synthesis of $\text{Cu}_{0.5}\text{Ba}_2\text{Ca}_2\text{Cu}_3\text{O}_{10-\delta}$ Precursor	24
3.2.2 Synthesis of $(\text{Cr})_x/\text{CuTi-1223}$ superconductor matrix	24
3.3 Characterization Techniques	25
3.4 X-ray diffraction (XRD)	26
3.4.1 X-rays production	26
3.4.2 Bragg's law	27
3.4.3 XRD Methods	28

3.4.4 Particle size determination.....	30
3.5 Scanning electron microscopy	31
3.5.1 Principle.....	31
3.5.2 Major components of SEM.....	32
3.6 Energy dispersive X-ray spectroscopy (EDX).....	33
3.6.1 Principle of EDX	34
3.6.2 Major components of EDX.....	34
3.7 LCR meter	35
3.7.1 Working of LCR meter.....	36
3.7.2 Advantages of LCR meter	36
3.8 Resistivity measurements.....	36
3.8.1 Measurement of resistivity by four probe method.....	37
CHAPTER 4	38
Results and Discussion.....	38
4.1 XRD Analysis	38
4.2 Resistivity measurement	39
4.3 Dielectric Properties.....	40
4.3.1 Real part of dielectric constant (ϵ').....	41
4.3.2 Imaginary part of dielectric constant	44
4.3.3 Dielectric loss Tangent	46
4.4 Conclusion.....	48
4.5 References.....	49

3.4.4 Particle size determination.....	30
3.5 Scanning electron microscopy	31
3.5.1 Principle.....	31
3.5.2 Major components of SEM.....	32
3.6 Energy dispersive X-ray spectroscopy (EDX).....	33
3.6.1 Principle of EDX	34
3.6.2 Major components of EDX.....	34
3.7 LCR meter.....	35
3.7.1 Working of LCR meter.....	36
3.7.2 Advantages of LCR meter	36
3.8 Resistivity measurements	36
3.8.1 Measurement of resistivity by four probe method.....	37
CHAPTER 4.....	38
Results and Discussion.....	38
4.1 XRD Analysis	38
4.2 Resistivity measurement	39
4.3 Dielectric Properties.....	40
4.3.1 Real part of dielectric constant (ϵ').....	41
4.3.2 Imaginary part of dielectric constant.....	44
4.3.3 Dielectric loss Tangent	46
4.4 Conclusion.....	48
4.5 References.....	49

List of Figures

Figure 1.1: Experimental data obtained in mercury by Gills Holst and H. KamerlinghOnnes in 1911.....	1
Figure1. 2: Superconductor at T_c when resistance is zero	2
Fig1. 3: Variation of critical temperature T_c (K) per year.....	4
Fig1. 4: The relationship between H_c , J_c and T_c	5
Fig1. 5 : Type I superconductor with applied magnetic field.....	6
Fig1. 6 : Representation of type II superconductor with applied field.....	7
Fig.1. 7 : Structure of CuTl-1223 unit cell.....	8
Fig.1. 8 : Phenomenology of cooper pairs formation.....	12
Fig.1. 9: Plate of capacitor with and without dielectric medium.....	13
Fig.1.10: Phenomenon of atomic polarization	14
Fig.1. 11: Representation of dipolar polarization.....	15
Fig.1. 12: Ionic polarization with and without applied field.....	15
Fig.1.13: pattern of interfacial polarization	16
Fig.1. 14: Structure of 0, 1, 2 and 3 dimension Nano materials.....	18
Fig.3.1: Synthesized chart of CuTl-1223	25
Fig.3.2: Synthesis of $(Cr)_x/CuTl-1223$ Nano particles	25
Fig.3.3: Schematic diagram for production of X-rays.....	27
Fig.3.4: Bragg's equation diagram	27
Fig3.5: Working diagram of rotating crystal method	29
Fig.3.6: Powder diffraction technique	29
Fig.3.7: Working diagram of transmission and back reflection Laue method.....	30
Fig. 3.8: Full width at half maxima	31
Fig. 3.9: Working diagram of Scanning electron microscope.....	32
Fig.3.10: Schematic diagram of EDX	34
Fig.3.11: LCR meter.....	36
Fig.3.12: Four probe technique	37
Fig.4.1: XRD of $(Cr)_x/CuTl-1223$ composites with (a) $x = 0$, (b) $x = 1.0$ wt.%.	39
Fig.4.2: Resistivity vs temperature measurements of $(Cr)_x/CuTl-1223$ nano-superconductor composite with $x = 0, 0.25, 0.5, 0.75$ and 1.0 wt. %.	40
Fig.4.3: (a-c): Real part of dielectric constant of $(Cr)_x/CuTl-1223$ nano-superconductor composite samples with different concentrations of Cr nanoparticles (a) 0 (b) 0.25% (c) 0.50% (d) 0.75% (e) 1.0 wt.%. (f) Variation of real part of dielectric constant	43
Fig.4.4(a-e): Imaginary part of dielectric constant of $(Cr)_x/CuTl-1223$ nano-superconductor composite samples with different concentrations of Cr nanoparticles (a) 0 (b) 0.25% (c) 0.50% (d) 0.75% (e) 1.0wt.%. In the inset there shown a variation of imagi	45
Fig.4.5(a-e): Dielectric loss tangent of $(Cr)_x/CuTl-1223$ nano-superconductor composite samples with different concentrations of Cr nanoparticles (a) 0 (b) 0.25% (c) 0.50% (d) 0.75% (e) 1.00 wt.%. In the inset there shown tangent loss vs temperature T	47

Abstract

Chromium (Cr) nanoparticles and $\text{Cu}_{0.5}\text{Tl}_{0.5}\text{Ba}_2\text{Ca}_2\text{Cu}_3\text{O}_{10-\delta}$ (CuTl-1223) superconductor were prepared separately by sol-gel and two steps solid state reaction method. Cr nanoparticles were mixed in appropriate ratios with CuTl-1223 matrix at the final stage to get $(\text{Cr})_x/\text{CuTl-1223}$ ($x = 0, 0.25, 0.5, 0.75,$ and 1.00 wt.%) nanoparticles-superconductor composites. Structure and phase purity of $(\text{Cr})_x/\text{CuTl-1223}$ composites were determined by XRD. XRD patterns of $(\text{Cr})_x/\text{CuTl-1223}$ showed that there was no change in crystal structure of host CuTl-1223 phase after addition of Cr nanoparticles, which provide a clue about the occupancy of these nanoparticles at the grains-boundaries. The dc-resistivity versus temperature measurements of these samples were carried out by four-probe technique. The zero resistance critical temperature $T_c (R = 0)$ of these samples was decreased by increasing wt. % of Cr nanoparticles in CuTl-1223 matrix due to magnetic nature of Cr particles. The dielectric properties of these samples i.e. dielectric constants ($\epsilon'_r, \epsilon''_r$), dielectric loss ($\tan\delta$) were determined by measuring the conductance (G) and capacitance (C) as a function of frequency at different operating temperatures. The values of dielectric parameters were decreased with the increase of frequency and become constant at higher frequency values, with the increase in temperature the real and imaginary part increase while the tangent loss decreases by increasing temperature. So the dielectric parameters can be tuned by the addition of Cr nanoparticles and with the variation of operating frequency and temperature.

Chapter 1

Introduction**1.1 Historical background of superconductivity**

Below a certain temperature some materials loss their resistance completely, this amazing phenomena is termed as superconductivity and the material that show such type of behavior are known as Superconductors. The first experiment was carried out by KamerlingOnnes in 1911[1]. On the basis of remarkable result of experiment, he concluded that resistance of mercury disappeared below 4.2 Kelvin temperature. In 1913 superconductivity of lead was estimated at 7 K, while in 1914 it was reported that Niobium Nitrate exhibits superconducting behavior at 16 K. Graphical representations of temperature versus resistance for mercury is shown in Fig. 1.1.

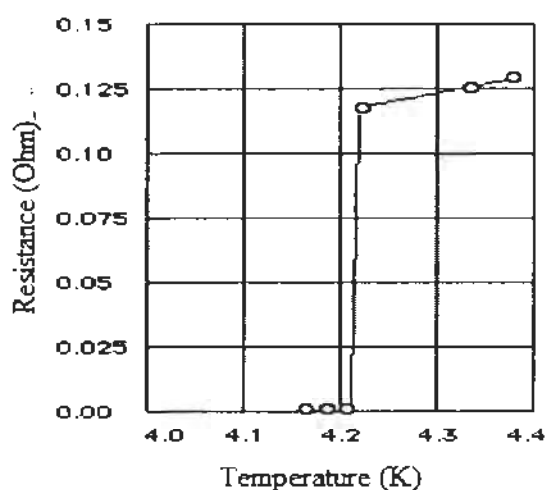


Fig.1.1: Experimental data obtained for mercury by Gills Holst and H. KamerlinghOnnes in 1911[2]

Many experimental works had been done to explain phenomenon of superconductivity. According to an important theory of Ochsenfield and Meissonier; superconductor totally destroys magnetic field at critical temperature. This effect is known as Meissner effect [3]. After Meissonier effect London explored a theory in 1935. London concluded that when material is in superconducting state all internal magnetic fields cease to exist. After London theory, in 1950, another famous theory was given by Ginzburg and Landau. In this theory they explained nanoscopic behavior of superconductors in effective way. This theory also categorized superconductors into two major types, namely as type-I and type-II. According to another theory that was given in 1957; the current in superconductor is due to a pairing phenomenon known as Cooper Pair. This famous theory is known as BCS theory [4].

1.2 Essential types of superconductivity

There are two major types of superconductivity.

- a) Zero resistance
- b) Perfect diamagnetism

1.2.1 Zero electrical resistance

Most important characteristic of superconductor is the disappearance of electrical resistance below a specific temperature known as critical temperature [5]. At zero resistance conductivity jumps to higher value and resistivity goes to zero as shown in Fig 1.2

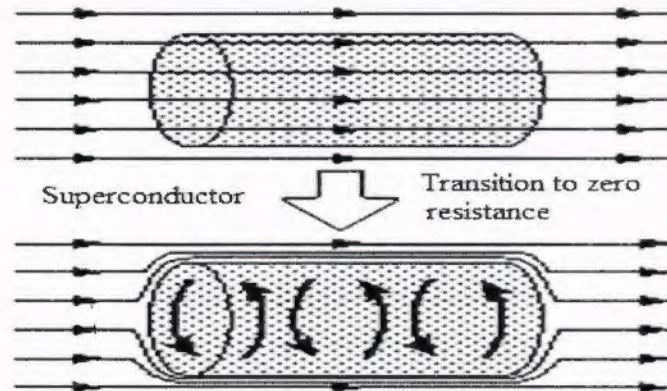


Fig. 1.2: Behavior of superconductor at T_c with zero resistance [6]

1.2.2 Perfect diamagnetism

This effect explains internal structure of superconductor in absence of field. Total value of current density is given by

$$J = J_{int} + J_{ext} \quad (1.1)$$

Magnetization M , which is produced by screening current, is defined as

$$\nabla \times M = J_{int} \quad (1.2)$$

According to theory of magnetic media magnetic field in terms of external currents is given by

$$\nabla \times H = J_{ext} \quad (1.3)$$

These three vectors M, H and B are related as

$$B = \mu_0 (H + M) \quad (1.4)$$

Maxwell equation tells us that $\nabla \cdot B = 0$

From above expression it can be seen that total magnetic field at the surface of conductor is equal to zero. So equation (1.4) becomes

$$M = -H \quad (1.6)$$

Moreover, magnetic susceptibility for superconductor is -1. This above explanation demonstrates the phenomenon of perfect diamagnetism [7].

1.3 Basic and important critical parameters of superconductors

The essential parameters for occurrence of superconductivity are given below

- a) Superconducting critical temperature
- b) Critical magnetic field
- c) Critical current
- d) Critical current density

1.3.1 Superconducting critical temperature

The resistivity reduces up to zero when material undergoes to a low temperature. For example resistivity of mercury vanishes completely at 4.2 K. At this point temperature is called critical temperature, which is denoted by T_c . Below critical temperature material is in superconducting state and above is T_c in normal state. Many materials exhibit superconducting properties at low temperature. Some materials also have high value of T_c , nearly equal to 92K. Variation of critical temperature per year is shown in Fig. 1.3.

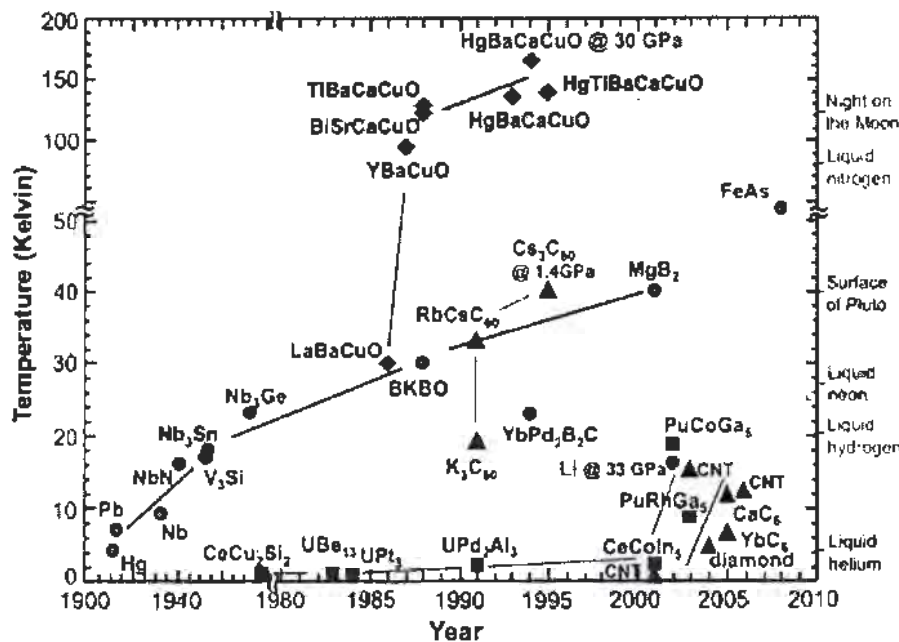


Fig. 1.3: Variation of critical temperature T_c (K) per year [8]

1.3.2 Critical magnetic field

At this stage value of magnetic field is called critical magnetic field. This value does not depend completely upon the temperature. Mathematical expression of critical magnetic field with temperature is given below

$$H_c = H_o \left[1 - \left(\frac{T}{T_c} \right)^2 \right] \quad (1.7)$$

Each superconducting material has a certain value of critical temperature (T_c) and critical magnetic field (H_c) [9].

1.3.3 Critical current

The maximum value of current at zero resistance is called critical current denoted by I_c . This phenomenon occurs abruptly in those materials which are not in pure form or refined. When current flows through a superconductor a magnetic field generates which reaches the value of critical magnetic field H_c . However, at H_c , superconductivity vanishes [10]. This type of superconductor is usually called Type-I superconductor. Poor conductors show superconducting properties at low temperature; while those which are good conductors e.g. copper, silver, have zero percent superconducting properties.

1.3.4 Critical current density

Large amount of current that flows through a superconductor per unit area is known as critical current density. When a material undergoes J_c then it shows superconducting behavior. Above J_c material's superconductivity terminates and it behaves as normal state.

1.4 Relation between Critical temperature, magnetic field and current density

These three basic parameters critical temperature T_c , critical magnetic field H_c , and critical current density J_c are largely depend on each other. These parameters also maintain their values below critical values to sustain material in superconducting state. The role of these parameters in superconductivity is demonstrated in Fig. 1.4. Shaded region shows superconducting behavior while non shaded region represents normal state of superconductor.

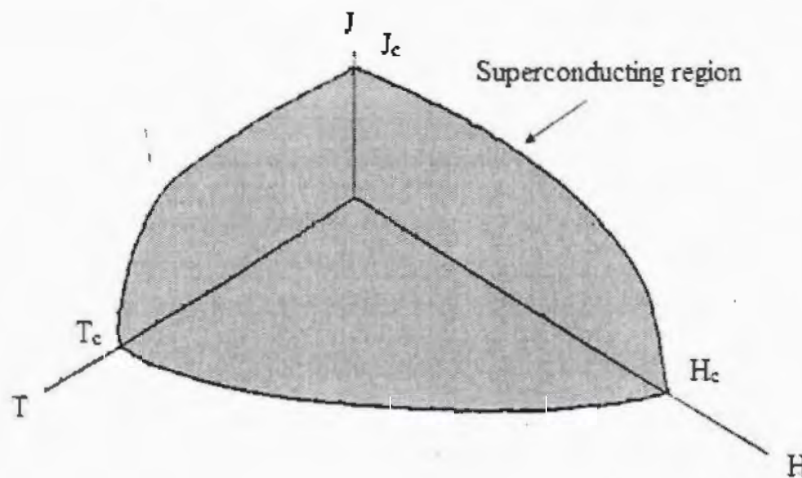


Fig. 1.4: The relationship between H_c , J_c and T_c [11]

1.5 Types of superconductors

A famous theory, which was given by Ginsburg and Landau in 1957 classifies two major types of superconductors; namely type-I and type II superconductors.

1.5.1 Type-I superconductors

In type-I superconductor a sudden change occurs in particular value of magnetic field called critical magnetic field denoted by H_c . There is only one specific value of critical magnetic field in type-I superconductor. In other words, the material undergoes from diamagnetic state to paramagnetic state. In type-I superconductor the maximum value of magnetic field is 0.2T. This value is small and this low value is one of the main drawback of type-I superconductor. Those

materials which have only one value of critical magnetic field are also known as soft magnetic materials [12]. Some pure materials such as silver, copper and gold behave similarly as type-I superconductor. The characteristics of type-I superconductor from non superconducting state to superconducting state are explained in Fig.1.4.

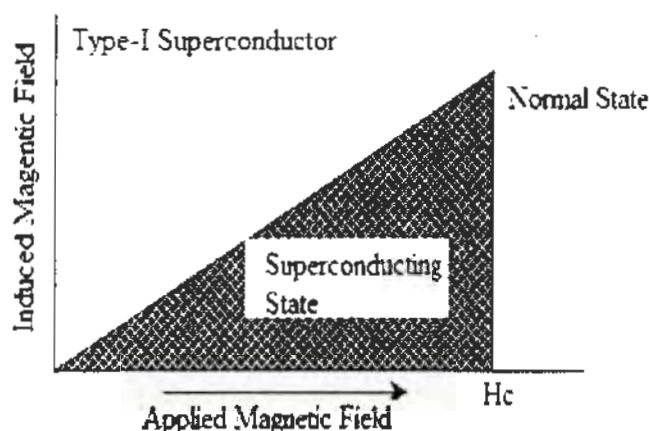


Fig. 1.5 : Type I superconductor with applied magnetic field [13]

1.5.2 Type- II superconductors

Transitions in type II superconductor are very different from type-I superconductor after when magnetic field is applied. The main difference in type-II and type-I superconductor is that there are two fields H_{c1} and H_{c2} ; because of these two fields, two phase transitions occur in type-II superconductors [14]. The concept of type-II superconductors was given by R.L.Shubnikov in 1935. On the basis of his theory of superconductivity, he was bestowed Nobel prize in 2003. High value of critical magnetic field in type-II superconductor is due to large amount of current. A plot of applied magnetic field versus induced magnetic field is shown in Fig.1.5 that practically demonstrates the behavior of type-II superconductor. Usually type-II superconductor also called hard superconductor. All compound and alloys are examples of type-II superconductors. In Type-II superconductors there are grain and grain boundaries due to compound element.

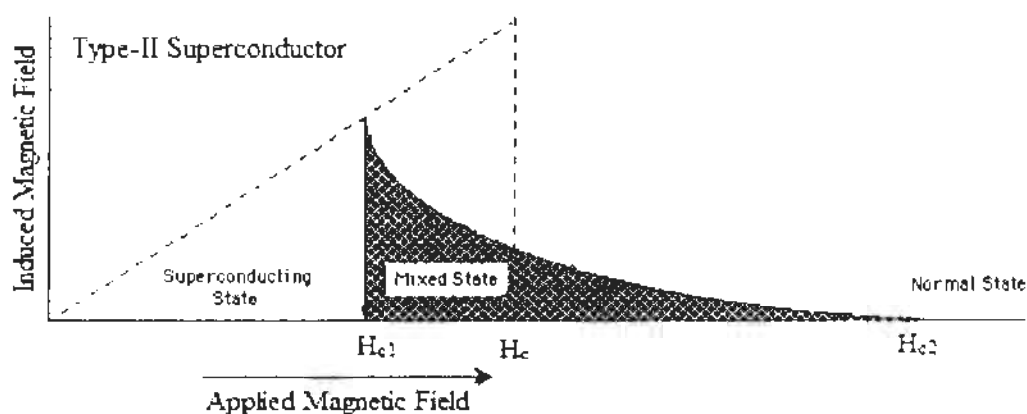


Fig. 1.6 : Representation of type II superconductor with applied field [13].

1.6 High temperature superconductors

Some specific materials which exhibit superconducting properties at high temperature are known as high temperature superconductors (HTSCs). First (HTSCs) discovery of high temperature was given by Bednorz and Müller in 1986 and they both shared noble prize for this exceptional work. They discovered, a superconductor whose critical value of temperature was nearly equal to 35K. In 2008, high temperature superconductors were also investigated for some materials like Yttrium Barium Copper Oxide (YBCO). Another Tl and Hg based superconductor with high value of critical temperature ranging between 125K to 134K, were made [15]. These high temperature superconductors were shapeless in terms of anisotropic behaviour with high value of critical current density J_c .

1.6.1 Tl-Ba-Ca-Cu-O superconductors

There are different compounds in CuTl-1223 high temperature superconductor. One of them is thalium (Tl) based and other one is copper (Cu) based. Hermann and Sheng explored the idea of CuTl superconductor first time. CuTl-1223 gained special attention due to its high superconducting properties such as low anisotropic, high critical value of temperature and current density. The important factor of this family is CuO_2 planes which are placed on each other one by one. Ca layers are specially used to connect CuO_2 planes. Oxygen coupling with Cu also play an important role to enhance the volume fraction of superconductors [16]. Schematic diagram of CuTl-1223 superconducting unit cell is shown in Fig. 1.6. Due to its high superconducting properties, CuTl-1223 has many practical applications.

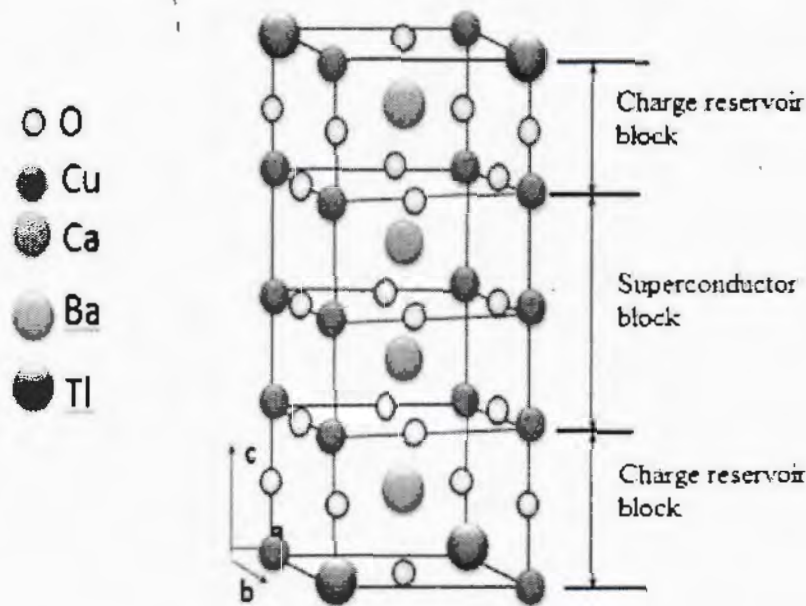


Fig.1. 7 : Structure of CuTl-1223 unit cell[17]

1.6.2 Hg-Ba-Ca-Cu-O superconductors

There is no major difference between Tl based superconductor and Hg superconductor in terms of structure. There are only a minute difference among these type of superconductors one is CuO_2 planes and other one is low critical value of Tl based superconductors as compared to Hg based superconductor. At atmospheric pressure value of critical temperture of Hg based superconductor is 134K. The superconductor that based on Hg is more sensetive because its pressure is direclty proportional to critical temperture. When pressure rises then value of critical temperture jumps up to 153K.

1.7 Experimental facts of superconductor

Some experimental facts of superconductors, which are very important for the phenomenolgy of superconductivity are described below.

1.7.1 Jospheson junction effect

This phenomenon of superconductivity was introduced by B.D. Jospheson in 1962 and is called Jospheson effect or weak superconductivity. The reason behind the name of weak superconductivity is that the two superconductors are weakly linked with each other. A thin dielectric is placed between the superconductors. The dielectire medium which is placed between the superconductors is very small e.g 2nm. A little current flows through the insulating gap.

There are two main types of Josephson junction effect, one is the A.C. Josephson junction effect and other one is D.C. Josephson junction effect.

1.7.2 A.C. Josephson junction effect

This is remarkable effect in superconductors. When DC current increases through weak links, voltage appears in the junction. So we conclude that after introducing DC we also get AC with frequency named as angular frequency represented by ω which is related as given below $\hbar\omega = 2V$ Where \hbar is equal to $\frac{h}{2\pi}$ and h is a plank's constant is equal to 6.63×10^{-34} JSec. ω is angular frequency equal to $2\pi f$. The symbol e is the charge on electron and V is voltage which appears in the junction.

1.7.3 D.C. Josephson junction effect

The amount of current passes through weak link (through a Josephson junction) is few amperes and passes through Josephson junction with no resistance even though material is an insulating material. This is one of the important properties of superconductor and is also known as coherence behaviour of electrons. At this stage Josephson junction electrons combine together in a single state. The weak link does not totally change the value of wave functions that are present in two sides of junction [18].

1.8 Meissner effect

Second important experimental fact for superconductor is Meissner effect. This effect is associated with amount of magnetic field that totally vanishes at superconductor state below critical temperature T_c . This is called Meissner effect which was given in 1933 by W. Meissner and R. Ochsenfeld. This effect is caused by magnetic flux of superconductor. It also explains that behaviour of superconductor is good as compared to an ideal conductor. After application of field to superconductor flux reduces to zero. The field that is produced due to superconducting current that also affects the applied field. The value of applied field does not change completely around the superconductor. This is the fabulous property of superconductor which is known as London penetration depth. Magnetic field is ejected when a normal type of conductor undergoes transition temperature [19]. Meissner tried to describe the complete theory of superconductivity.

1.9 Important theories of superconductivity

There are some important theories that demonstrate the phenomenon of superconductivity differently e.g. London theory. It was given by two brothers Hertz and Fritz in 1935. After

London theory, another theory that explains microscopic mechanical behaviour of superconductivity was given by Ginzburg and Landau. In 1957 another famous theory was explored by J. Bardeen, L.N. Cooper and J.R. Schrieffer. This theory explains the microscopical behaviour of superconductivity, which is based upon a Cooper pair.

1.9.1 London theory

London theory is based upon two fluids models. One is named as normal fluids, which have density n_n and the other one is known as superconducting electrons represented by n_s . Summation of these gives us the total amount of density fluids as in equation 1.9.

$$n = n_n + n_s \quad (1.8)$$

Also there is an influence of n_s having density in the superconducting state and n_n in the normal state. Mathematical models for both states are

$$T \rightarrow T_c, n_n \rightarrow 0 \text{ \& } n_s \rightarrow \text{max or } (T < T_c) \text{ (for non-superconducting state)}$$

And

$$n_s \rightarrow 0, n_n \rightarrow \text{max as } T \rightarrow T_c \text{ for } (T > T_c) \text{ (for superconducting state)}$$

The correlation between electric current, electric field and magnetic field introduced by London which is called the London equation. London equations are

$$\frac{\partial J_s}{\partial t} = \frac{n_s e^2}{m} E \quad (1.9)$$

$$\nabla \times J_s = -\frac{n_s e^2}{mc} B \quad (1.10)$$

In these models

" n_s " is the density of superconductor, " m " is the mass of electron, " e " is electronic charge, " J_s " is superconducting current density, " E " is electric field, " B " is magnetic field.

1.9.2 London penetration depth

Theoretical effect for Meissner effect firstly described by two brothers London and Fritz. According to Meissner effect when field is applied into superconductor, it enters the sample by some specific length equal to 2nm , this specific length is called London penetration depth.

1.9.3 BCS Theory

To describe behaviour of superconductivity quantum mechanically, a famous theory was given by Bardeen, Cooper and Schrieffer in 1975 and is known as BCS theory [20]. According to this theory the phenomenon of superconductivity is due to electron pair known as Cooper pair. Formation of electron-electron interaction is shown in Fig. 1.9. This theory also explained the isotope effect i.e. $T_c \propto M^{-\alpha}$. In the above expression M is ionic mass of crystal lattice and α is isotopic element. Value of isotopic element is less than or equal to $\frac{1}{2}$.

When current flows through superconductor, electrons experience a force of attraction near a core which contains positive charge. Due to this special phenomenon a distortion is produced in the lattice and as a result the value of energy in the lattice reduces. This is done near the lattice and is caused by phonons. The attractive force between electrons is due to reduction in energy. The momentum between electrons is also opposite and this attractive force is too much stronger than Coulomb's attraction at certain temperature. This phenomenon is known as Cooper pairs. These pairs are treated as a single wave function and strongly depend on the motion of each other. When current flows in the form of Cooper pairs, no scattering phenomenon occurs and the value of resistivity goes to zero. As we know, when resistivity is negligible then conductivity reaches to a higher level in that material. There are some specific materials that have good conducting properties and these are not valid for superconductivity e.g. silver, gold and copper because there is an excess of free electrons so electron-lattice vibration is not available.

Three consequences of BCS theories are

- (i) Attractive force between electrons are due to coupling between electron-phonon interaction. (Bardeen)
- (ii) Just two electrons near Fermi surface (isolated two electrons) (Cooper).
- (iii) Near the Fermi surface all electrons are in the form of pair state. (Schrieffer)

Combination of above three consequences is called BCS theory.

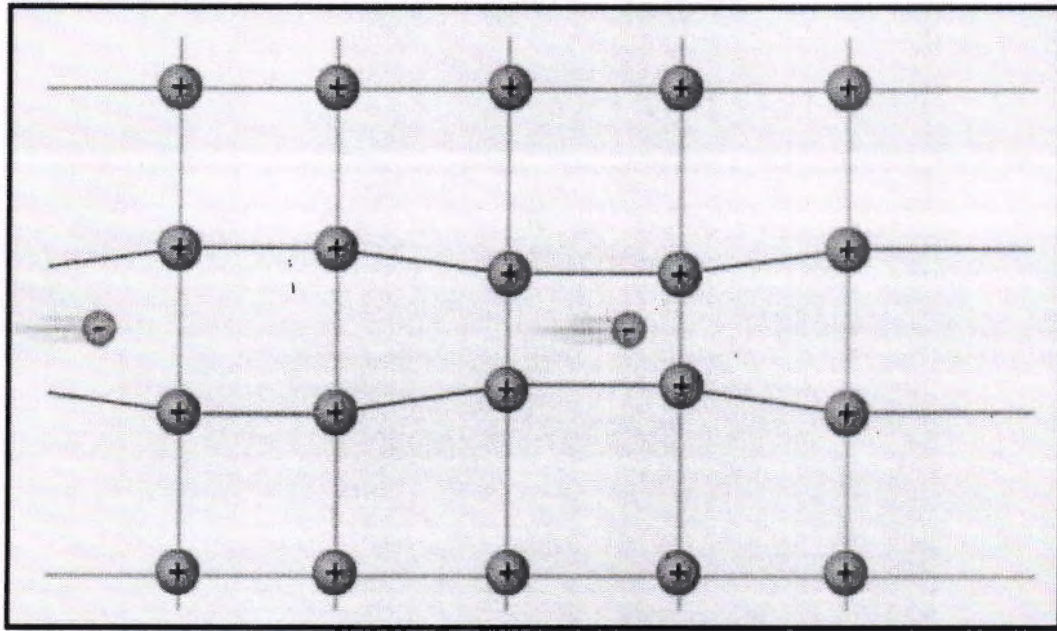


Fig.1. 8 :Phenomenology of cooper pairs formation[21].

1.11 Introduction to dielectric materials

From periodic table, it can be seen that there are three types of elements named as conductors that has excess of free electrons, secondly insulators also known as dielectrics that do not conduct electricity due to tightly bound electrons and third one state is intermediate between conductors and insulators named as, semi conductors.

We will discuss here insulating medium which is also known as dielectric. From energy band theory it can be seen that there is a large gap between valence and conduction band nearly equal to 5eV in case of insulator so the electrons in the valence band can not jump to the empty conduction band due to this large gap. In contrast to insulator there is no gap between valence and conduction bands in conductors. However, in semiconductors there is a narrow gap between valence and conduction bands e.g 1eV. When a conductor is placed between positive and negative terminal of the battery, current flows from it. But when insulator is inserted between them, then current does not flow due to tightly bound electrons and hence electric polarization takes place[22]. Due to phenomenon of electric polarization, a charge is slightly displaced from its original position. When dielectric is placed between the plates of capacitor then capacitance increases and also energy and charge stored between the plates rises. Representation of capacitor with and without dielectric medium is shown in Fig. 1.10.

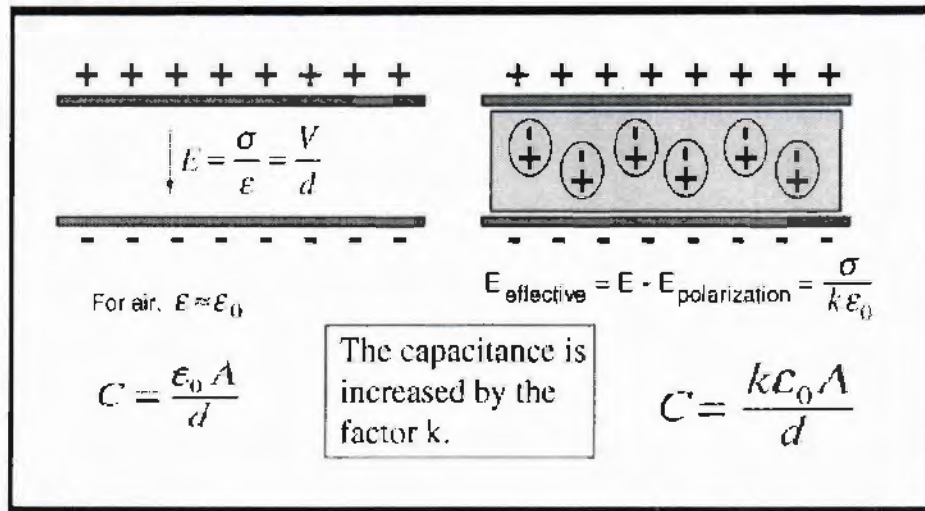


Fig.1. 9: Plate of capacitor with and without dielectric medium [23].

From above figure it can be seen that when insulating medium is placed between the plates of capacitor, then capacitance is increased by factor K .

1.11.1 Dielectric polarization

Dielectric polarization is defined as “dipole moment per unit volume”. Mathematical expression of dielectric polarization is

$$P = \frac{\sum p}{V} \quad (1.11)$$

From a dielectric model, a dielectric material has two kinds of charges namely positive and negative charges. These charges are bound in dielectric material[24]. When electric field is disconnected then atoms go to their original position. The time for which atoms regain their original position is called relaxation time. When dielectric material is under influence of electric field then polarization takes place which actually tells us the behaviour of that material. Parallel plate capacitor is one of the best example of dielectric polarization. When insulated material is placed between the plates and potential difference is applied between the plates of capacitor, plates get charge. Normally when value of potential difference increases it enhances capacitance because capacitance varies inversely with potential. Value of capacitance increases by a factor ϵ_r known as constant called dielectric constant or relative permittivity of free space. Mathematical expression of capacitance is

$$C = \frac{Q}{V} \quad (1.12)$$

Dielectric constant is also defined as Ratio of capacitance when insulator is placed between the plate of capacitor to the plate of free space i.e.

$$\epsilon_r = C / C_0 \quad (1.13)$$

1.12 Classification of polarization

There are four types of polarizations which are described below one by one.

1.12.1 Atomic polarization

An atomic structure contains equal amount of positive and negative charges and it is in neutral state. Nucleus is central part of atom which contains only positive charge inside and electrons revolve around the nucleus in any dielectric material. When a nucleus is subjected under the influence of electric field then nucleus moves towards the field where as electrons move away from the field. This type of polarization is known as atomic polarization and takes place between the frequency ranges 10^{10} to 10^{13} MHz. Atomic phenomenon with and without electric field is shown in Fig. 1.10.

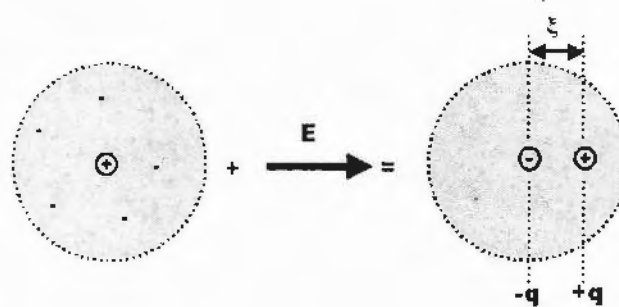


Fig.1.10: Phenomenon of atomic polarization[25]

1.12.2 Oriental (Dipolar polarization)

This phenomenon takes place at the frequencies ranges between 10^3 to 10^9 Hz. There are some specific materials that have a fixed value of dipole moment. The molecules of these materials are usually in form of very small tiny dipoles. Water and ceramics are the best examples of dipolar molecules. When dielectric material is under influence of electric field, the materials move towards the applied field. Oriental polarization is shown in Fig 1.11.

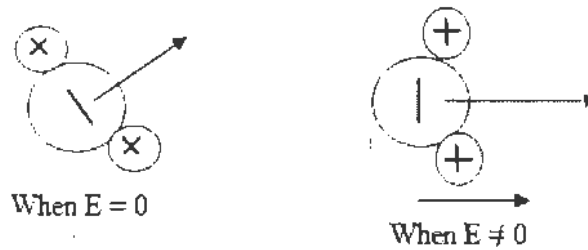


Fig. 1.11.: Representation of dipolar polarization [26]

1.12.3 Ionic polarization

The influence of electrostatic force holds ions having different nature usually these are in ionic bond. When field is applied to the molecules then some poles are generated having equal and opposite charges separated by a distance. Such types of polarization which are due to positive and negative ions are called ionic polarization. Figure 1.12 demonstrates separation of positive and negative ions. Displacement between the bonds depends upon the temperature.

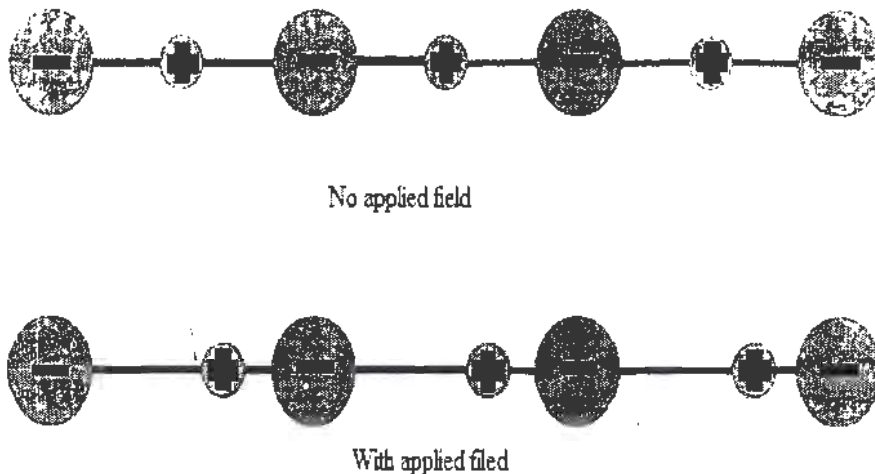


Fig.1. 11: Ionic polarization with and without applied field [26].

1.12.4 Interfacial polarization

This type of polarization is more sensitive and takes place in the low frequency ranges e.g. 10^3 Hz and it may increase to few kilohertz. Interfacial polarization usually occurs in irregular shape (amorphous). After applied field, charges gather in both sides of crystal in irregular manner and in opposite direction called electrodes. Fig.1.15 shows pattern of irregular and opposite charges. Interfacial polarization occurs due to diffusion of charges.

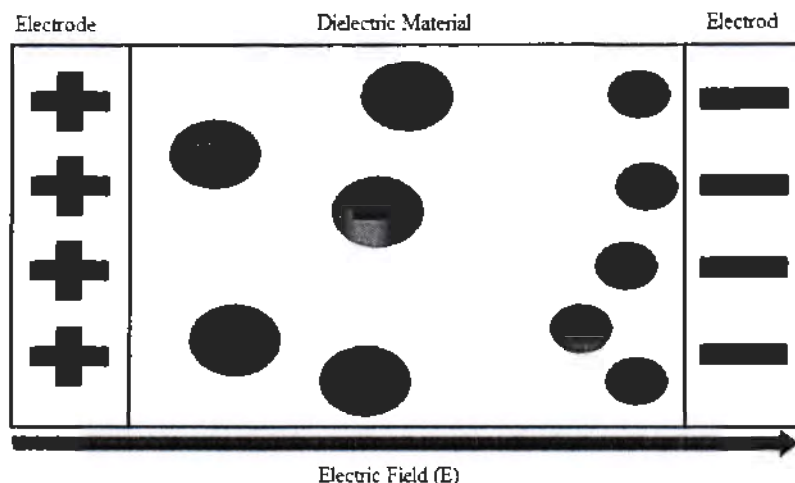


Fig.1.12:pattern of interfacial polarization[26]

1.13 Temperature dependent polarization

Only one type of polarization depends upon the value of temperature that is the interfacial polarization. In interfacial polarization, some dipoles are fixed. For gases this type of polarization varies inversely with the temperature. When amount of temperature increases then interfacial polarization reduces. Same phenomenon happens in liquids. As temperature rise then polarization decreases. Due to enhancement of polarization we get total polarization.

1.13.1 Frequency dependence of dielectric polarization

When frequency (A.C field) is applied to insulating material (dielectric), then charges slightly move from their original position. Due to slight displacement, there is a formation of pole with opposite charges separated by a small distance known as dipole [27]. Due to ionic behavior ionic and dipolar polarization do not show good response against field.

1.14 Classification of dielectric materials

A dielectric material categorized in different parts depends upon its values of frequency and temperature [28]. These parts are described below.

1.14.1 Real part

When external field is applied to the dielectric material that is placed between the plates of capacitor. Some part of energy stores between the plates due to influence of applied field. This is due to effect of dipolar polarization at less value of frequency and temperature, and is known as real part which is denoted by ϵ' . Mathematical expression for real part of dielectric is

These structures consist between molecules and infinite bulk system. Suitable control of properties and response of Nano structures can lead new device and technology.

1.16 Nonmaterial's categories

There are various categories of materials based upon their dimensions described as follows

1.16.1 Zero dimensional (0-D) Nano materials.

All those materials that contain all dimensions less than one hundred Nano meters (100nm) are called zero dimensions. Most of these Nano particles are spherical in size. Clusters are the best example of zero dimensions.

1.16.2 One dimensional (1-D) Nano materials

Those materials which are equal to Bohr radius, that is, motion of hole and electrons confined into two directions. Lengths of these materials are in micrometer but diameter is only few nanometers. Examples of one dimension Nano materials are Nano tubes and Nano rods etc.

1.16.3 Two dimensional (2-D) Nano materials

Those materials which have two sides in bulk sides and one side at Nano Scale are called two dimensions. Nano materials e.g. Films and Layers. Area of these materials is large but, thickness is small.

1.16.4 Three dimensional (3-D) Nano materials

No dimension is in nano meter range e.g. having all sides in bulk materials.

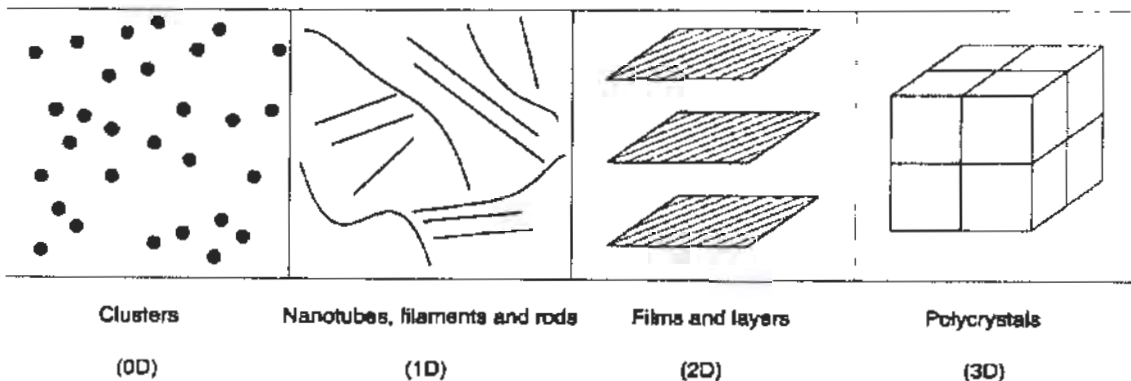


Fig.1. 13: Structure of 0, 1, 2 and 3 dimensional Nano materials[30]

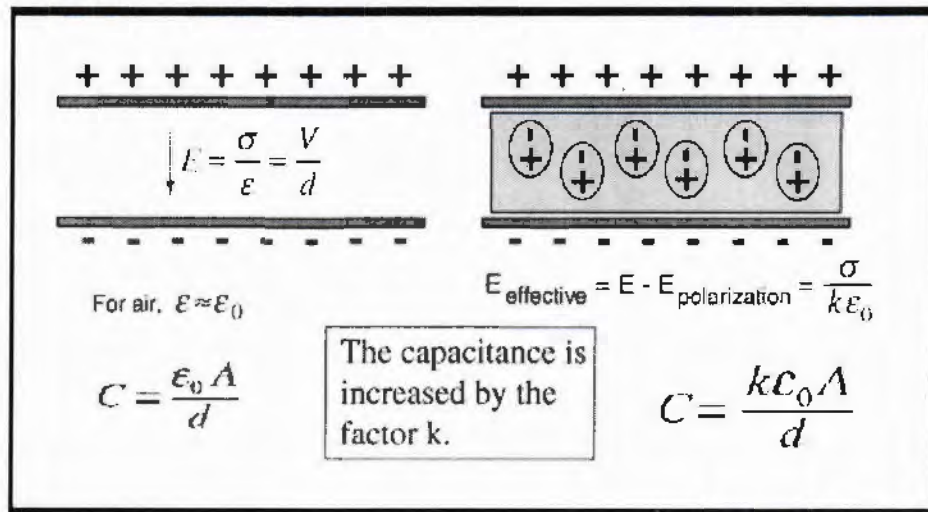


Fig.1. 9: Plate of capacitor with and without dielectric medium [23].

From above figure it can be seen that when insulating medium is placed between the plates of capacitor, then capacitance is increased by factor K .

1.11.1 Dielectric polarization

Dielectric polarization is defined as “dipole moment per unit volume”. Mathematical expression of dielectric polarization is

$$P = \frac{\sum p}{V} \quad (1.11)$$

From a dielectric model, a dielectric material has two kinds of charges namely positive and negative charges. These charges are bound in dielectric material[24]. When electric field is disconnected then atoms go to their original position. The time for which atoms regain their original position is called relaxation time. When dielectric material is under influence of electric field then polarization takes place which actually tells us the behaviour of that material. Parallel plate capacitor is one of the best example of dielectric polarization. When insulated material is placed between the plates and potential difference is applied between the plates of capacitor, plates get charge. Normally when value of potential difference increases it enhances capacitance because capacitance varies inversely with potential. Value of capacitance increases by a factor ϵ_r known as constant called dielectric constant or relative permittivity of free space. Mathematical expression of capacitance is

$$C = \frac{Q}{V} \quad (1.12)$$

Dielectric constant is also defined as Ratio of capacitance when insulator is placed between the plate of capacitor to the plate of free space i.e.

$$\epsilon_r = C / C_0 \quad (1.13)$$

1.12 Classification of polarization

There are four types of polarizations which are described below one by one.

1.12.1 Atomic polarization

An atomic structure contains equal amount of positive and negative charges and it is in neutral state. Nucleus is central part of atom which contains only positive charge inside and electrons revolve around the nucleus in any dielectric material. When a nucleus is subjected under the influence of electric field then nucleus moves towards the field where as electrons move away from the field. This type of polarization is known as atomic polarization and takes place between the frequency ranges 10^{10} to 10^{13} MHz. Atomic phenomenon with and without electric field is shown in Fig. 1.10.

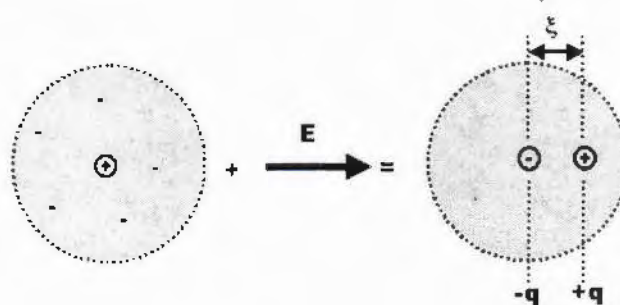


Fig.1.10: Phenomenon of atomic polarization[25]

1.12.2 Oriental (Dipolar polarization)

This phenomenon takes place at the frequencies ranges between 10^3 to 10^9 Hz. There are some specific materials that have a fixed value of dipole moment. The molecules of these materials are usually in form of very small tiny dipoles. Water and ceramics are the best examples of dipolar molecules. When dielectric material is under influence of electric field, the materials move towards the applied field. Oriental polarization is shown in Fig 1.11.

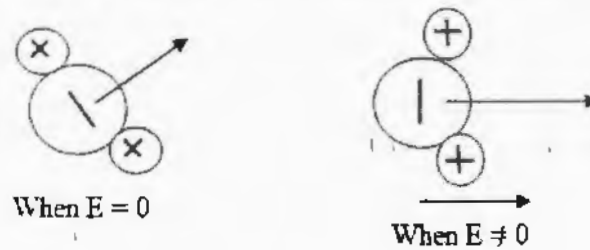


Fig. 1.11.: Representation of dipolar polarization [26]

1.12.3 Ionic polarization

The influence of electrostatic force holds ions having different nature usually these are in ionic bond. When field is applied to the molecules then some poles are generated having equal and opposite charges separated by a distance. Such types of polarization which are due to positive and negative ions are called ionic polarization. Figure 1.12 demonstrates separation of positive and negative ions. Displacement between the bonds depends upon the temperature.

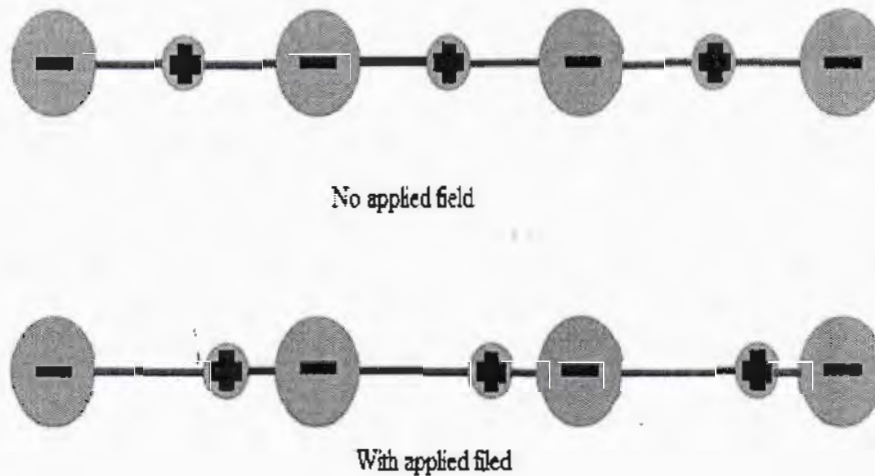


Fig.1. 11: Ionic polarization with and without applied field [26].

1.12.4 Interfacial polarization

This type of polarization is more sensitive and takes place in the low frequency ranges e.g. 10^3 Hz and it may increase to a few kilohertz. Interfacial polarization usually occurs in irregular shape (amorphous). After applied field, charges gather in both sides of crystal in irregular manner and in opposite direction called electrodes. Fig.1.15 shows pattern of irregular and opposite charges. Interfacial polarization occurs due to diffusion of charges.

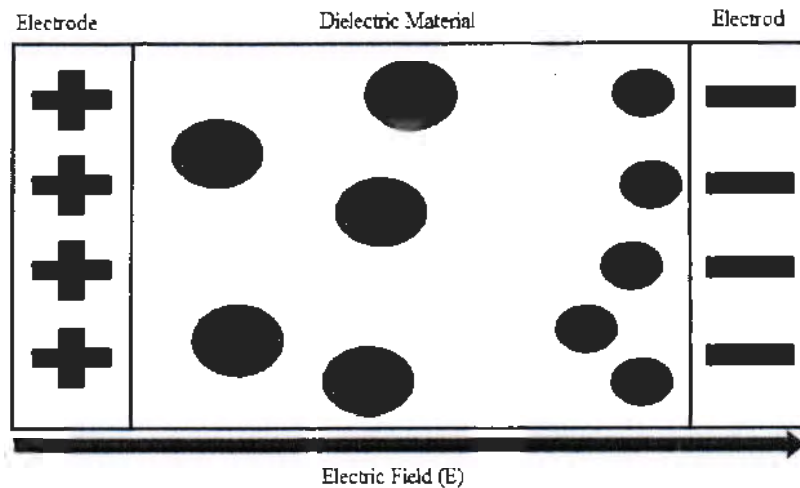


Fig.1.12: pattern of interfacial polarization [26]

1.13 Temperature dependent polarization

Only one type of polarization depends upon the value of temperature that is the interfacial polarization. In interfacial polarization, some dipoles are fixed. For gases this type of polarization varies inversely with the temperature. When amount of temperature increases then interfacial polarization reduces. Same phenomenon happens in liquids. As temperature rise then polarization decreases. Due to enhancement of polarization we get total polarization.

1.13.1 Frequency dependence of dielectric polarization

When frequency (A.C field) is applied to insulating material (dielectric), then charges slightly move from their original position. Due to slight displacement, there is a formation of pole with opposite charges separated by a small distance known as dipole [27]. Due to ionic behavior ionic and dipolar polarization do not show good response against field.

1.14 Classification of dielectric materials

A dielectric material categorized in different parts depends upon its values of frequency and temperature [28]. These parts are described below.

1.14.1 Real part

When external field is applied to the dielectric material that is placed between the plates of capacitor. Some part of energy stores between the plates due to influence of applied field. This is due to effect of dipolar polarization at less value of frequency and temperature, and is known as real part which is denoted by ϵ_r' . Mathematical expression for real part of dielectric is

$$\epsilon_r' = \frac{Cd}{A\epsilon_0} \quad (1.14)$$

In above expression, C is constant known as capacitance of capacitor, d is the separation between the plates; A is area of each plate ϵ_0 is constant known as permittivity of free space.

1.14.2 Imaginary part

When dielectric material is subjected under the influence of field; some amount of energy losses between the plates. Imaginary part of dielectric arises due to lagging factor of polarization with applied field. Real part becomes smaller with increasing amount of frequency. This type is called imaginary part and denoted by ϵ_r'' . Mathematical expression for imaginary part is

$$\epsilon_r'' = \epsilon_r' \tan \delta \quad (1.15)$$

1.14.3 Tangent Loss (Tan δ)

Ratio of energy loss to energy stores when dielectric material is inserted between the plates this ratio is known as tangent loss and denoted by Tan δ . Tangent loss tells us about behavior of conduction and dielectric relaxation. By increasing the value of temperature, tangent loss also goes up but usually inversely with frequency. Mathematically we write tangent loss as

$$\text{Tan}\delta = \epsilon_r''/\epsilon_r' \quad (1.16)$$

1.14.4 Ac conductivity

Charges show slightly displacement after material is under influence of electric field this phenomenon is known as AC conductivity. AC conductivity acts inversely with temperature particularly at low value of frequency. Mathematically it can be written as

$$\sigma_{ac} = \omega\epsilon_r\epsilon_0\tan\delta \quad (1.17)$$

ϵ_0 is constant known as permittivity of free space.

1.15 History of Nanotechnology

The historical idea of nanotechnology is given, traditionally, after dinner speech given by Richard Feynman at the American society on Dec. 29, 1959 with a revolutionary sentence said by him that, "There is a plenty of room at the bottom".

Nanotechnology deals with synthesis, characterization and exploration of nanostructure materials [29]. These materials are characterized at least one dimension in the Nano meter range.

These structures consist between molecules and infinite bulk system. Suitable control of properties and response of Nano structures can lead new device and technology.

1.16 Nonmaterial's categories

There are various categories of materials based upon their dimensions described as follows

1.16.1 Zero dimensional (0-D) Nano materials.

All those materials that contain all dimensions less than one hundred Nano meters (100nm) are called zero dimensions. Most of these Nano particles are spherical in size. Clusters are the best example of zero dimensions.

1.16.2 One dimensional (1-D) Nano materials

Those materials which are equal to Bohr radius, that is, motion of hole and electrons confined into two directions. Lengths of these materials are in micrometer but diameter is only few nanometers. Examples of one dimension Nano materials are Nano tubes and Nano rods etc.

1.16.3 Two dimensional (2-D) Nano materials

Those materials which have two sides in bulk sides and one side at Nano Scale are called two dimensions. Nano materials e.g. Films and Layers. Area of these materials is large but, thickness is small.

1.16.4 Three dimensional (3-D) Nano materials

No dimension is in nano meter range e.g. having all sides in bulk materials.

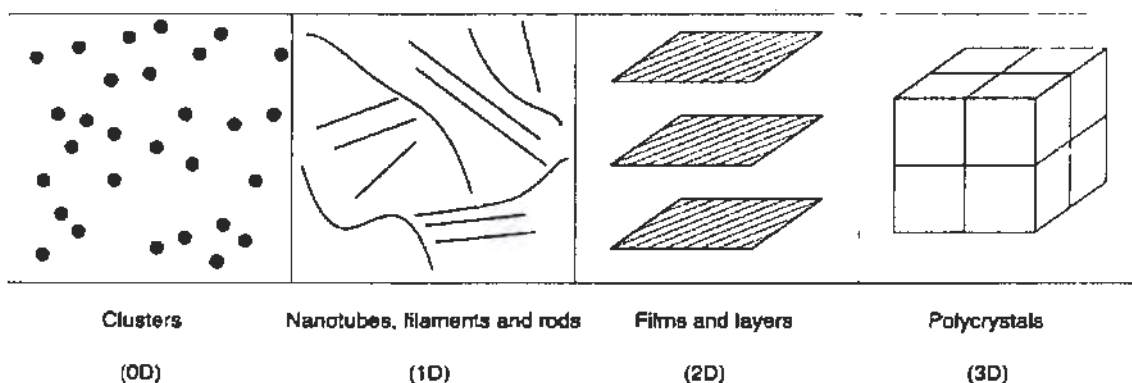


Fig.1. 13: Structure of 0, 1, 2 and 3 dimensional Nano materials[30]

Chapter 2**Literature review**

N. T. Cherpaket et al. [31] concentrated the likelihood of utilizing semi optical dielectric resonators energized with higher kind of motions for the estimation of high T_c superconductor surface impedance. The upsides of the resonators are clear, in that they permit examination and non-damaging testing of HTSC made in plate shape from materials of various mixes and structure over a wide recurrence extend. High reproducibility of the outcomes was acquired utilizing the picked strategy. Cases of complex investigations of HTSC in the millimeter and radio frequency range are given in the review.

Y. Takahashi et al. [32] explored impacts of La-doping on crystallinity and dielectric properties of $\text{SrAl}_{0.5}\text{Ta}_{0.5}\text{O}_3$ films for high- T_c superconductor. La-SAT film on c-hub situated YBCO movies indicate grid constriction and a lessening of its dielectric constant with expanding the La-doping proportion to $x \cong 0.1$. The La solvency confine exists in the x extends in the vicinity of 0.1 and 0.2, and the La-SAT changes to have arbitrary introduction at x of 0.2, despite the fact that its dielectric properties turn out to be still better. It was additionally affirmed that the superconducting properties of La-YBCO films developed on La-SAT with $x \leq 0.1$ are practically equivalent to those for the case without La-doping.

C. Bernhard et al. [33] studied the dielectric conduction of the high T_c cuprate superconductors by synchrotron light source. They set up that the vast brightness of a synchrotron light source empowers one to perform extremely exact ellipsometric estimations even on rather little single precious stones of the cuprate high T_c superconductors (HTSCs). They demonstrated how the phenomenal electronic anisotropy of this compound impacts the ellipsometric spectra, that gets under touching recurrence. From the anisotropy corrected spectra we have recognized different constrained segments which contrast with IR-dynamic in-plane delighted phonon modes broad one which we associate with a total electronic mode. They showed data exhibit that the technique of far-infrared ellipsometry engages one to secure low down finding out about the low-imperativeness IR-dynamic excitations, even inside seeing a strong response as a result of the free charge transporters.

S. Çavdaret et al. [34] studied the dielectric properties of Bi based vanadium substituted superconductor at different concentrations of vanadium, different test frequencies and temperatures were studied. Melt quenching method was used for the synthesis of these

superconductors. Frequency and temperature dependence of dielectric properties were studied. The increase in dielectric constant (ϵ') is small at higher frequencies but at low frequency the change in dielectric constant is more prominent. The range of frequency was kept 10 kHz to 10 MHz and temperature range was taken 80K to 300 K. The dc electrical resistivity (ρ) and ac electrical conductivity (σ_{ac}) measurements of vanadium added superconductors were also investigated which proves that critical temperature suppresses as vanadium is substituted in sample. Negative capacitance (NC) was also investigated which was due to polarization effect.

G. N. Pandey et al. [35] carried out studies on Omni directional reflectance properties of superconductor-dielectric photonic crystal. The calculated band structure and reflectance/transmittance of the periodic structure of superconductor-dielectric materials are observed with maximum reflection. The band gaps and reflectances/transmittances of the structure at the various angles of incidence are found to shift toward higher normalized frequency range. The enlarged band gaps and reflectance of the structure with the increased angle of incidence was because of property of the Bragg gaps. Such quality of the superconductor-dielectric periodic structure may be applied to construct the broad band reflector that can be used in low temperature region.

M. Mumtaz et al. [36] investigated the impacts of oxygen post-strengthening on the superconducting and dielectric properties of $\text{Cu}_{0.5}\text{Tl}_{0.5}\text{Ba}_2\text{Ca}_3(\text{Cu}_{4-y}\text{Cd}_y)\text{O}_{12-8}$ superconductor tests. In all oxygen post-tempered specimens the negative capacitance was watched. The adjustment in the dielectric parameters after oxygen present tempering was said on be the confirmation of the variety in O_8 oxygen of charge store layer that controls the stream of bearers towards the leading CuO_2 planes. At customary state temperature, the warm tumult is higher and polarizability is lower creating diminishing of dielectric steady and increment in dielectric misfortune consider. A well-assembled dielectric scattering is seen at low frequencies and temperatures and the invert impacts are seen on dielectric properties at hoisted temperatures and frequencies. They watched varieties in the dielectric parameters of tests emphatically rely on upon the working temperature and recurrence of the outer connected air conditioning field. The dielectric conduct of the materials can be synchronized by the oxygen post-toughening accordingly of which the variety of oxygen substance in the structure of the materials controls the bearer's thickness. In this way, the oxygen post-toughening can be utilized to tune the

recurrence and temperature dependent dielectric properties of $\text{Cu}_{0.5}\text{Tl}_{0.5}\text{Ba}_2\text{Ca}_3(\text{Cu}_{4-y}\text{Cd}_y)\text{O}_{12-\delta}$ superconducting tests.

K. Yoshii et al. [37] looked into dielectric properties of Bi_2CuO_4 at frequency ranging from 1kHz to 1MHz. There was monotonic decrease in dielectric constant with increasing frequency of applied field such behaviour was referred as dielectric dispersion. This was because of lacking of spatial coherence of dielectric response. Tangent loss express for activation energy, it suggested that electron hopping between Cu ions were responsible for the dielectric response

T. Li et al. [38] probed the effect of NiO-doping on the microstructure and dielectric properties of $\text{CaCu}_3\text{Ti}_4\text{O}_{12-x}\text{NiO}$ ceramics using SEM, Raman spectra and dielectric spectrum measurements. The positron annihilation lifetime spectra were used to study the effects of defects on the dielectric characteristics. The results of SEM showed the variations of grain morphology by raising NiO content. A suitable content of NiO can assist the grain growth, which is useful to develop the dielectric properties in a $\text{CaCu}_3\text{Ti}_4\text{O}_{12}$ (CCTO) structure. Positron end results show that there are vacancy-type defects are there in the sample and the concentration of the defect and the defect variety both change with raising NiO content. The main findings are significance of grain morphology and the properties of defects in controlling the electrical properties of above sample or ceramic.

A. Biscnet al. [39] examined dielectric properties of the $\text{Ba}_{1-x}\text{La}_{2x/3}\text{ZrO}_3$ compound. XRD, FTIR and Raman examination demonstrated that there is no stage move occurring in the pieces between $x = 0$ and 0.1wt.%. XRD examination demonstrated that because of lower radii of La^{3+} than Ba^{2+} unit cell volume and grid parameters are slowly smothered with raising La^{3+} content. Despite that Raman examination proposed the arrangement of higher level of symmetry with raising La^{3+} content. This was ascribed to changes in metal–oxygen separate in the material. The expansion of oxygen opportunities due to consolidation of La^{3+} substance into the BaZrO_3 grid brought on abatement in band hole. The dielectric steady was measured by Hakki–Coleman strategy. The microwave dielectric consistent diminished with increment of La^{3+} substance. DRA thinks about demonstrate that the reverberation recurrence and data transfer capacity rely on the permittivity of the materials which can be connected in different fields of correspondence.

K. Y. Tan et al. [40] investigated dielectric properties of MgB_2 . The examples with a follow measure of protecting MgO stage demonstrated negative dielectric permittivity because of

their metallic conduct. As the sintering temperature was expanded, the crystallinity and grain availability were enhanced prompting a more negative dielectric permittivity. The specimens sintered at higher temperature additionally indicated higher A.C conductivity at low recurrence and a faster decline of conductivity at higher recurrence ascribed to the expanded powerful mass of charge transporters. Therefore, those examples indicated higher and a more fast dielectric loss.

M. Mumtaz et al.[41] tried different things with Zinc oxide (ZnO) nanoparticles incorporation in CuTi-1223 superconducting stage. The incorporation of ZnO nanoparticles was found to diminish the voids and to enhance the between grains network in the host CuTi-1223 stage. The dielectric properties of these examples i.e. dielectric constants (real and imaginary part), and dielectric misfortune ($\tan \delta$), were controlled by tentatively measuring the capacitance (C) and conductance (G) as an element of recurrence at various working temperatures. The estimations of dielectric parameters were diminished with the expansion of recurrence and wind up noticeably steady at certain higher recurrence esteems, while the estimations of these parameters were expanded with the increment of working temperature esteems. Thus, we can tune the dielectric properties of CuTi-1223 superconducting stage by fluctuating the substance of ZnOnano-particles, recurrence and working temperature.

S. K. Hodak et al. [42] fabricated coplanar capacitors and their dielectric behavior is investigated in frequency range of 1 MHz to 2 GHz and temperature ranges from 300K to 400 K. They used off-axis pulsed laser deposition technique to prepare Epitaxial strontium titanate (SrTiO_3) thin films on neodymium gallate (NdGaO_3) substrate at 820 C°temperature. Ti/Au coplanar capacitors electrodes with 25 μm gap separation, gap width of 1.5 mm and overall size used was 3mm, synthesized by photolithography and evaporation method. Dielectric properties were enhanced by lowering surface to volume ratio and increasing in-plane grain size.

Chapter 3

Synthesis and Characterization Techniques

3.1 Synthesis techniques

3.1.1 Solid State Reaction method

There are two steps of solid state reaction method which are described below one by one as follows.

(a) One-Step method

One of the simplest synthesis techniques is one step method. The powder which is in the form of elemental oxide changed to obtain appropriate amount of thallium Tl. This technique was found to be very easy as compared to other techniques such as; multi step method which is explained below.

(a) Multi-Step method

There are series of methods to obtain superconducting matrix. Multi step method is conducted at different temperatures. In this method firstly, element introduced and then mixed separately. Multi step method gives a lot of advantages, no loss of amount of thallium and melting result at very low temperature. As carbonates have many physical properties, so it is usually used for synthesis of high temperature superconductor. Above the value of 900°C and advantage of carbonates that carbonates completely disappeared. To avoid these losses a method which is named as solid state reaction method is used which is divided into two steps: Firstly, carbonates and copper oxide that (CuO_2) mixed with one another above 900°C and secondly, thallium oxide that varied at low temperature.

3.2 Sample preparation method

3.2.1 Synthesis of $\text{Cu}_{0.5}\text{Ba}_2\text{Ca}_2\text{Cu}_3\text{O}_{10-\delta}$ Precursor

CuTi-1223 superconductors were synthesized by a famous method named as solid state reaction method. Figure 3.1 shows the method of synthesizing of CuTi-1223 superconductors. Compounds $\text{Ba}(\text{NO}_3)_2$, $\text{Ca}(\text{NO}_3)_2$ and $\text{Cu}(\text{CN})$ were taken with suitable ratios and mixed with one another. After mixing compounds were grounded with mortar and then further pelletized. After that this mixture of appropriate ratios placed in furnace at value of temperature 860°C for 24 hours. When time is completed then switched off the furnace and waited for room

temperature. After 24 h heat treatment, the material was again ground for 1 h and loaded in quartz boats for second time heat treatment under similar conditions

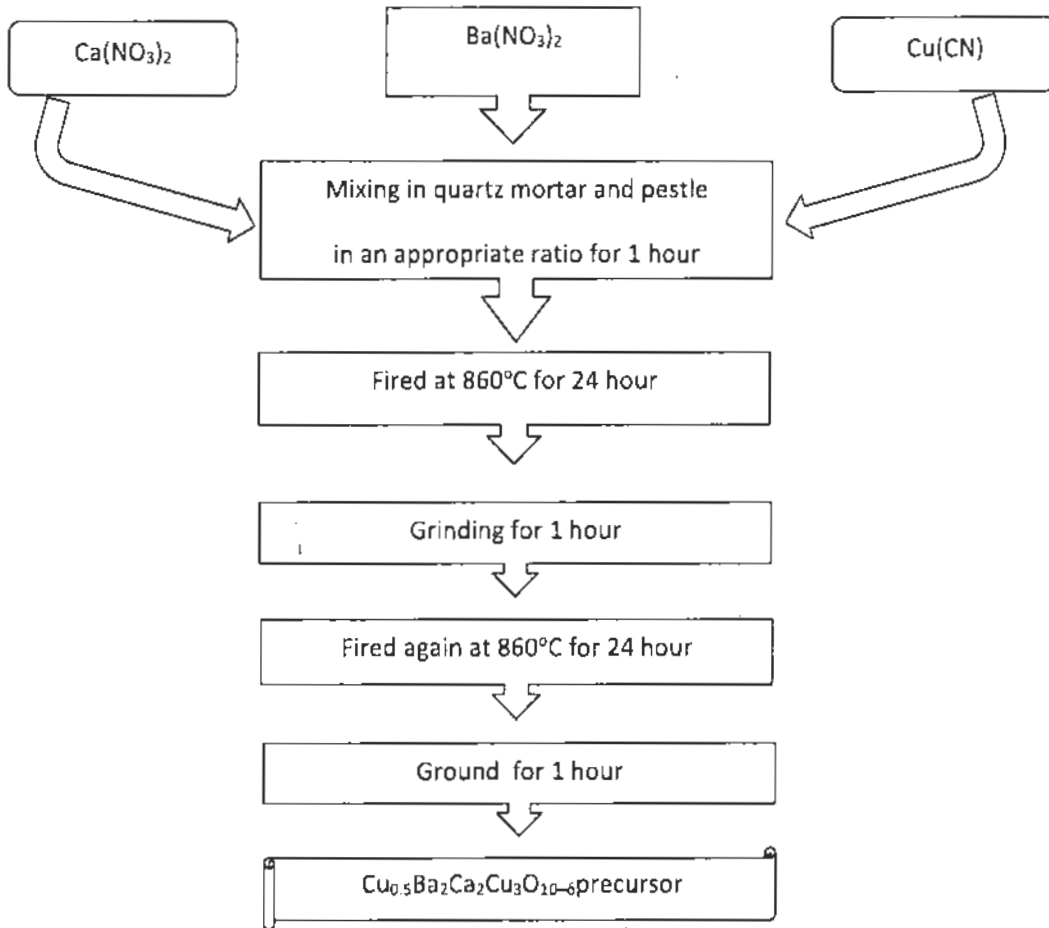


Fig.3.1: Synthesized chart of CuTI-1223

3.2.2 Synthesis of $(Cr)_x/CuTI-1223$ nano- superconductor composites

After synthesis of CuTI-1223 superconductor matrix now included chromium Nano particles $(Cr)_x$ having different values of x and Tl_2O_3 . Resultant matrix formed after inclusion of Cr which was $(Cr)_x/CuTI-1123$ again grounded for one hour. Now using hydraulic press made pellets of resultant superconducting composites at value of $3.8\text{tons}/\text{cm}^2$. Pellets that are made must wrapping gold capsule and again placed in furnace at temperature nearly equal to 860°C for 10 minutes [43, 44]. This process can also be explained with the help of diagram as shown in figure.

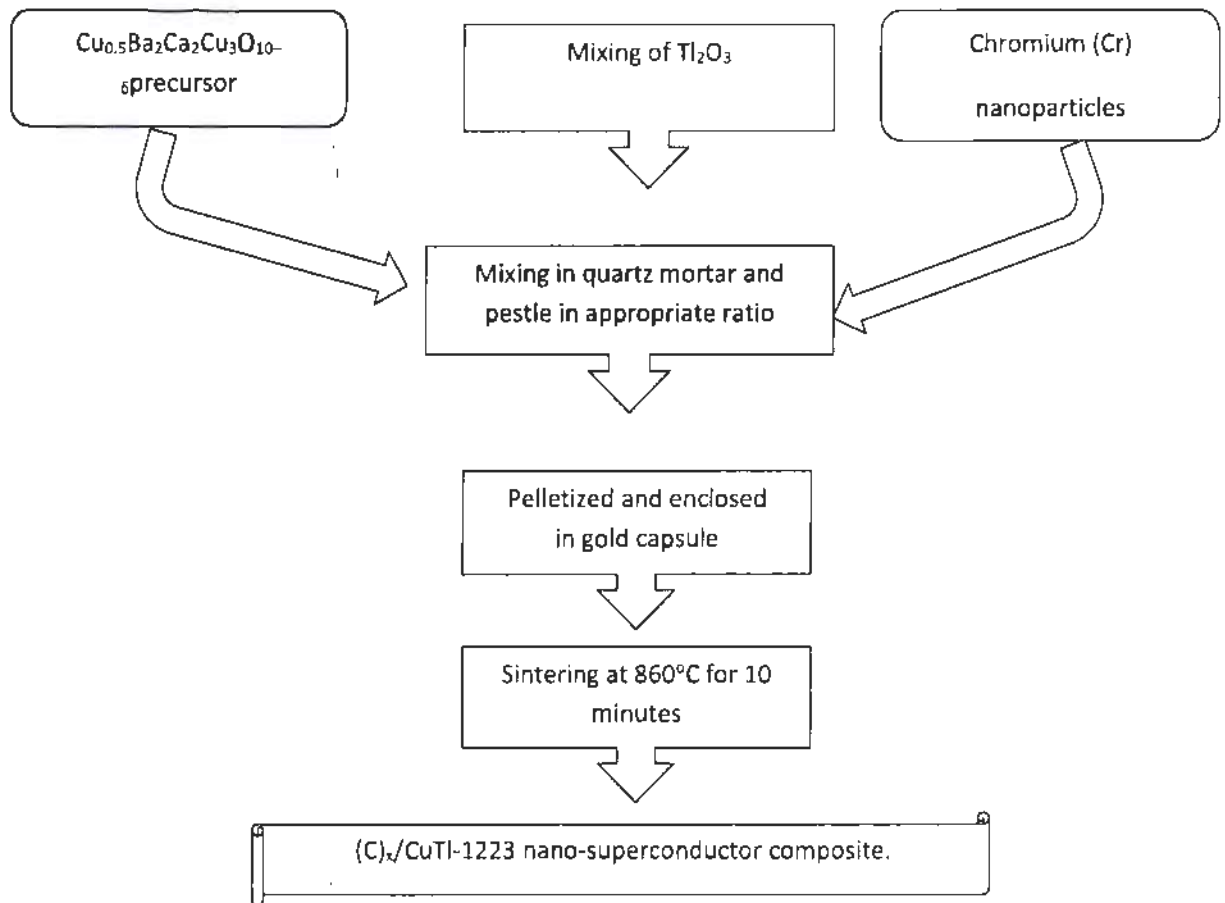


Fig.3.2: Synthesis of (Cr)/CuTI-1223 Nano particles

3.3 Characterization Techniques

There are several techniques which are being used here:

- (a) X-ray diffraction(XRD)
- (b) Scanning electron microscopy (SEM)
- (c) Energy dispersive X-ray spectroscopy(EDX)
- (d) Dielectric measurement by LCR meter

XRD is used for sample phase purity and crystalline structure. Scanning electron microscopy (SEM), which is used for chemical deposition of sample and EDX is used for elemental analysis. These techniques are discussed one by one below.

3.4 X-ray diffraction (XRD)

One of the most powerful techniques is XRD which is specially used to identify the crystalline phases which are present in the sample. This technique also used for different structural properties such as structural defects, phase composition and epitaxial etc. Thickness in thin films and atomic structure in irregular materials is also determined through XRD technique [45]. This technique is non-contacting as well as non-destructive, due to these reasons this technique is considered as ideal for insitu studies. Materials that can be used with any element can be studied through this technique. In this technique X-ray beam with wavelength from 0.7 to 2°A are used for diffraction [46].

3.4.1 X-rays production

When a beam of electrons bombarded on a metal surface then due to collision of electrons with atoms fast moving electrons are decelerated. In other words electrons losses amount of energy in the form of tiny bundles which are simply known as photon. These resultant photons which contain high amount of energy are called X-rays. This effect is called braking radiation (bremsstrahlung) or continuous X-rays spectrum. The intensity of X-rays varies inversely with the amount of frequency. The maximum value of energy which is produced by X-rays photon is product of potential and electronic charge that is eV . There is another type of X-rays which is called characteristics X-rays. In this type of X-rays electrons knock out from inner surface and a vacancy is created in the inner shell. Continuous X-rays spectrum usually produced emission spectrum at constant value of frequency.

Usually, X-rays produced through a X-rays tube which is also called vacuum tube. High voltage is used to heat up filament to produced electrons which are accelerated to high velocities. Schematic diagram of production of X-rays is shown in the Fig. 3.3.

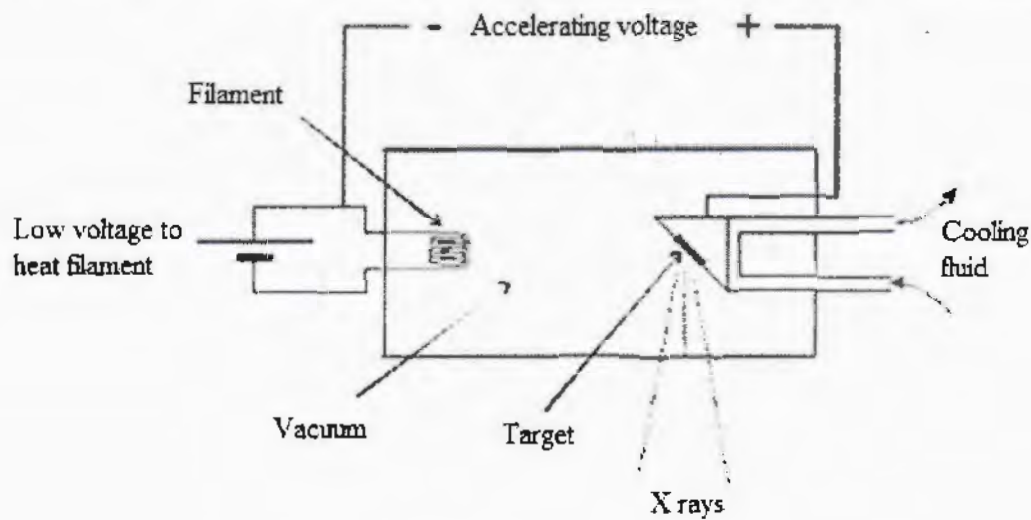


Fig.3.3: Schematic diagram for production of X-rays[47]

Accelerated electrons collide with metal surface which is usually in the form of tungsten. After collision with tungsten disc, reflection of these electrons in the form of photons which are actually X-rays.

3.4.2 Bragg's law

Crystal structure having constant wavelength when bombarded with X-rays at specific angles these incident X-rays are getting reflected and wavelength shows behaviour of constructive interference. For constructive interference path difference must be equal to intergral multiple of wavelength. At this special condition a beam of X-rays diffracted which is equal to incident beam as shown in figure.

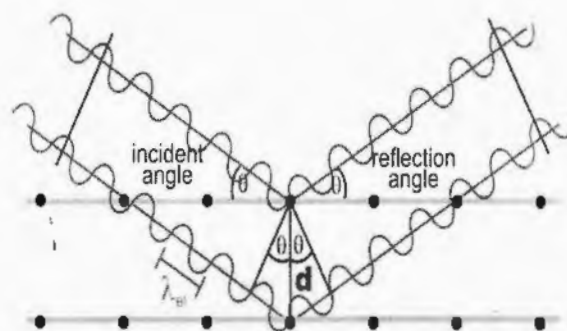


Fig.3.4: Bragg's equation diagram[48].

Bragg gave relation between wavelength of incident x-rays , angle which is known as angle of incidence and seperation between the planes as follows:

$$2d\sin\theta = n\lambda \quad (3.1)$$

The above relation known as Bragg's law. Here, d is seperation between planes, n is order, θ is angle known as diffraction angle and λ is called simply wavelength.

3.4.3 XRD Measurements techniques

There are several XRD techniques that are

- (a) Rotating crystal method
- (b) Powder diffraction method
- (c) Laue method

(a) Rotating crystal method

In rotating crystal method a monochromatic beam of X-rays used within a single crystal. The axis of single crystal is normal to beam of monochromatic X-rays. This whole system is covered with a cylindrical film. When a single crystal rotate within the cylindrical film for incident beam that is monochromatic, give right values of Bragg angles and after that a beam is found which is diffracted. One of the main advantage of rotating crystal method is determination of unknown crystal sturcture. Also from rotating crystal method after recorded of diffracted beams, shape and size arrangement of sample present inside the crystal can be determined. Rotation of crystal gives the lattice planes at some pionts and maling accurate value for Bragg angle. Duc to this rotation of crystal this method is known as rotating crystal method. Working diagram of rotating crystal method is shown in the Fig.3.5 given below.

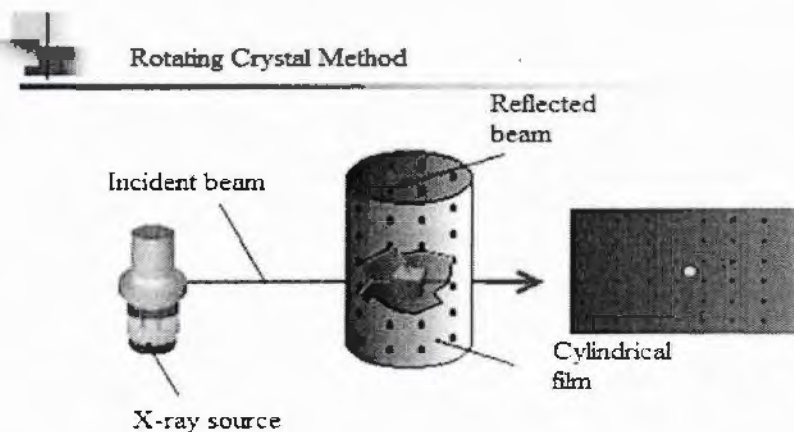


Fig.3.5: Working diagram of rotating crystal method [49]

(b) Powder diffraction method

Second important X-rays diffraction technique is powder diffraction method. This technique is used for structure characterization of material. In this technique if an instrument performing a powder measurements then this is also called powder diffractometer. Powder diffraction technique is also called single diffraction technique[50]. Working diagram of powder diffraction method is shown in the Fig. 3.6.

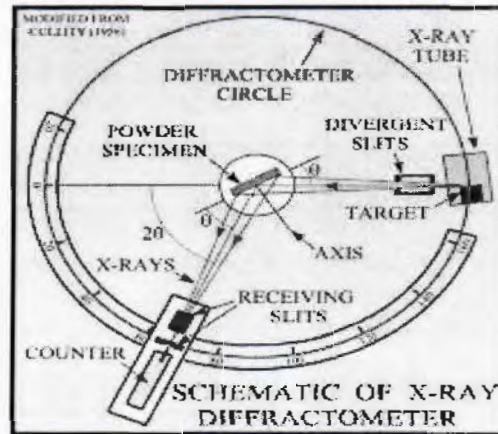


Fig.3.6: Powder diffraction technique[51]

In powder diffraction technique constructive interference only takes place for those certain values of diffracted angle and wavelengths which fulfill Bragg conditions. This technique is useful if the value of material is 1mg. If, more than one phase then it is difficult to determine the phase of material by this method.

(c) Laue method

One of the oldest technique of XRD is Laue method. This method is mostly useful for determination of large single crystal. Reflection radiation which is in white colour transmitted through a crystal. There are mainly two types of Laue method one is black reflection method and other one is transmission method. In black reflection method film is placed between X-ray source and crystal. Some beams that are reflected in backward direction are noted. Resultant film is in the hyperbolic form which is shown in figure. In transmission Laue method beams are recorded when film is placed in the back side of crystal. Resultant film cut the beam and diffraction is finally in the form of elliptical shape.

TH: 18282

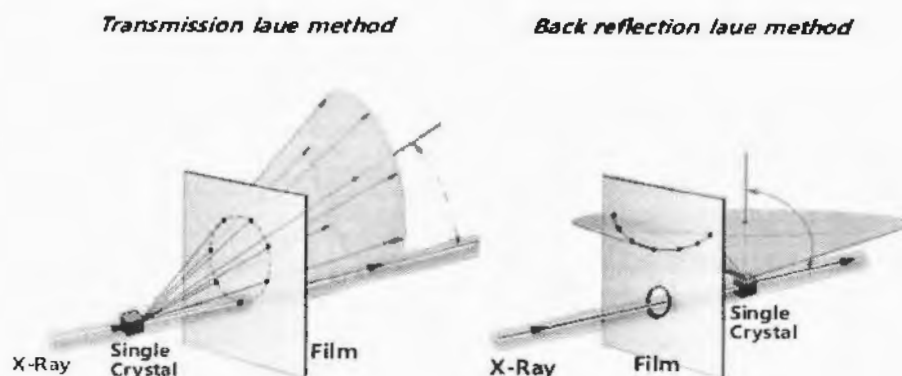


Fig.3.7: Working diagram of transmission and back reflection Laue method [52]

3.4.4 Particle size determination

A formula which was given by Paul Scherrer in 1918 is used to find the size of particles. Through Debye Scherrer formula measurement of grain size can be done which is nearly equal to 0.1 to 0.2mm. Mathematically

$$D = \frac{K\lambda}{\beta \cos\theta} \quad (3.2)$$

Here D is required particle size. In the above expression K is Scherrer constant for cubic crystal value of K is 0.94 and λ is wavelength for X-rays. β is full width of half maximum which is in radian and θ is known as Bragg's law as shown in Fig. 3.8.

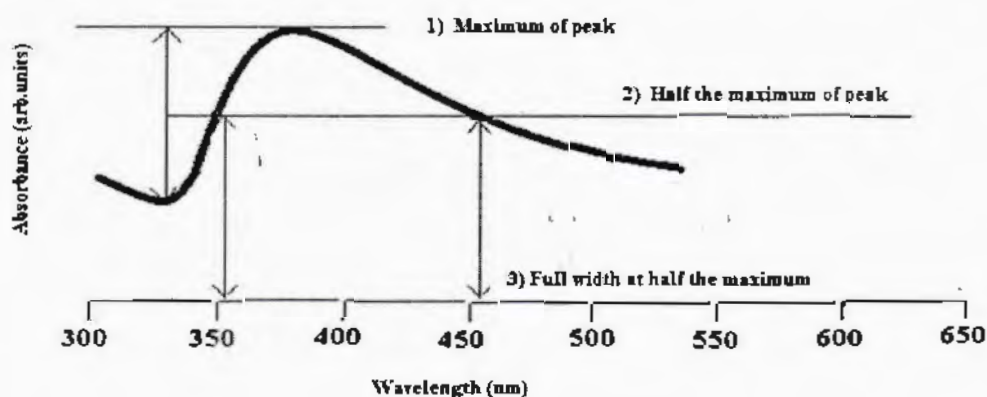


Fig.3.8: Full width at half maxima [53]

3.5 Scanning electron microscopy (SEM)

After scanning sample with beam of electrons a microscope that produces images is known as scanning electron microscope. Scanning electron microscopy gives information about composition and topography of sample. Through SEM resolution achieved is nearly equal to 1nm. Observations of specimen can be obtained in high and low vacuum also in wet conditions. This technique also gives us special resolution images and spatial variations chemical composition.

3.5.1 Principle

The electrons that are accelerated in scanning electron microscopy contain suitable value of kinetic energy, this suitable amount of energy produces variations of electrons with sample. After collision these electrons are decelerated and dissipation of energy signal is found. These signals also include some spatial characteristics that secondary electrons actually give us scanning electron microscopy images, back scattered electrons that are used for determination of crystal structure. Surface morphology and topography of a sample is shown through secondary electrons [54]. For composition of a multi phase sample shown using back scattered electrons. Schematic diagram of SEM is shown in Fig. 3.9. Scanning electron microscope is also called non destructive technique because in this technique collision of electrons with sample not affected the sample that are under consideration. Due to these reasons we check morphology of sample again and again.

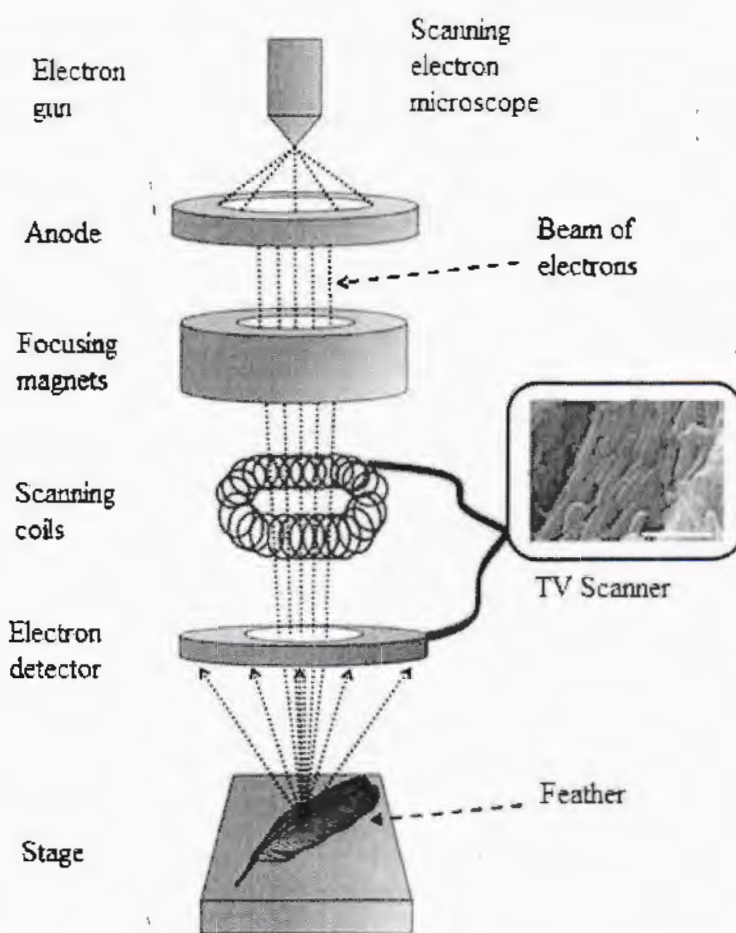


Fig.3.9: Working diagram of Scanning electron microscope [55]

3.5.2 Major components of SEM

There are several major components of scanning electron microscope

- (a) Electron gun
 - (b) Lenses
 - (c) Scanning coils
 - (d) Sample chamber
 - (e) SEM detector
 - (f) Back scattered electrons
- (a) Electron gun

Electrons are produced through electron gun by thermionic emission. The voltage that produces electrons is between 1 to 40KV. The beam of electrons is produced with a tungsten wire having a sharp tip value equal to 100nm.

(b) Lenses

The narrow electron beams are focused with the help of condenser lens. This smaller beam of electrons is narrow which easily contacts with the surface of the sample.

(c) Scanning coil

These coils are used to focus the beam in X and Y-axis after beam being focused by scanning coils the electrons are actually focused in the form of beams.

(d) Sample Chamber

The sample is placed inside the chamber after mounting. This sample chamber has rotation devices, temperature stages, optical cameras and many other devices that actually help in imaging the sample.

(e) SEM detector

The electrons which are coming from the sample detected through a detector called SEM detector. There are mainly two types of electrons used in SEM for imaging that are secondary electrons and back scattered electrons. These electrons are also called low energy electrons escaped from the surface of the sample by imaging. One of the detectors in SEM is called "Everhart Thornley" detector. After that amplification signal is read through monitor.

(f) Back scattered electrons

High energy electrons in SEM are called back scattered electrons. These electrons collide with sample and after that move in back direction. In other words electrons collision is elastic. These electrons are scattered in back direction in well-manner that's why detector gives compositional information about sample. Detector controls the contrast and also gives us topographical information.

3.6 Energy dispersive X-ray spectroscopy (EDX)

Elemental analysis and chemical composition of a sample can be determined through a technique which is named as energy dispersive X-ray spectroscopy and sometime also called as energy dispersive X-ray analysis (EDXA). To study the emission of a type of X-rays which is characteristics X-rays from a specimen a beam of charged particles or a beam of X-rays is focused into the sample. From a sample data EDX give different peaks for different elements.

EDX also gives information about imaging phenomenon. Schematic diagram of EDX is shown in the figure. EDX also give us qualitative analysis of a sample. Working diagram of energy dispersive X-ray spectroscopy is shown below.

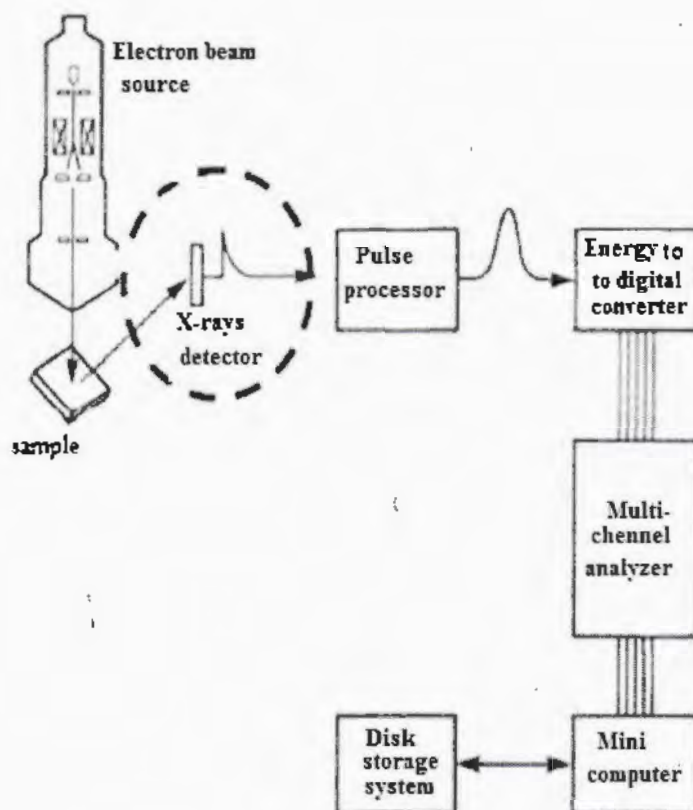


Fig.3.10: Schematic diagram of EDX[56]

3.6.1 Principle of EDX

Each element has its own atomic structure which gives unique emission spectrum. This is the basic principle of energy dispersive X-ray spectroscopy.

3.6.2 Major components of EDX

There are four major components of energy dispersive X-ray spectroscopy. These are as follows:

1. Electron or X-ray beam (Excitation source)
2. X-ray detector
3. Pulse processor

4. Pulse analyzer

To obtain the phenomenon of characteristics X-rays a high energy beam of electrons also called beam of X-rays is collided with the sample which is under consideration. At normal state electrons are bound. Incident beam may excite electrons from inner shell creating a hole in the replacement of electron. Difference between two states realised in the form of energy which are simply X-rays. The amount of energy which is measured by an instrument called energy dispersive spectrometer. After these measurements next step is to measure the composition of sample which is under consideration. Then finally in pulse processor the specimen is analyzed in pulse analyzer to obtain photographic picture of actual composition. In energy dispersive X-ray spectroscopy each element has a specific wavelength of characteristic X-rays on the basis of which these elements are differentiated from each other.

3.7 LCR meter

An electronic instrument which consists of an inductor (L), capacitor(C) and resistor(R) is known as LCR meter. Through this instrument we can measure inductance, capacitance and resistance of an electronic circuit. Inductance is due to causing voltage in a current in the circuit capacitance is used to store amount of charge and third component which is resistance always oppose the amount of current that flows in an electronic circuit. Through LCR meter measurements are taken between 100Hz to 10 KHz frequency ranges [57]. For capacitance measurements source used is D.C whose value is nearly equal to 40V. Schematic diagram of LCR meter is shown in the Fig.3.11.



Fig.3.11: LCR meter[58]

3.7.1 Working of LCR meter

Working of LCR meter consists of following steps:

- (i) The component which is used to examine is under influence of A.C voltage source.
- (ii) Through LCR meter voltage and current are measured initially.
- (iii) From measured values of voltage and current we can easily calculate impedance.
- (iv) From LCR meter we easily assumed series and parallel arrangements.
- (v) For LR measurements always placed in series while for RC measurements always placed in parallel.

3.7.2 Advantages of LCR meter

There are several advantages to use LCR meter. These are mentioned below

- (i) This is very simple method for operation.
- (ii) Through LCR meter measurements are possible with very minor error.
- (iii) This is ideal instrument having quality control.
- (iv) LCR meter used for both analogue and digital quantities.

3.8 Resistivity measurements

From statement of Ohm's law if value of voltage and current are known then resistance of the substance is;

$$R = \frac{V}{I} \quad (3.3)$$

This resistance of substance is proportional to length of conductor and varies inversely to area of conductor that is given mathematically as follows

$$R = \rho \frac{L}{A} \quad (3.4)$$

Where ρ is resistivity of the substance which can be written from above expression as follows;

$$\rho = R \frac{A}{L} \quad (3.5)$$

Here R is resistance of specimen L is length and A is cross sectional area. Where ρ is resistivity.

3.8.1 Measurement of resistivity by four probe method

For measurement of resistivity a technique is used which is called as four probe technique. Four probe techniques are used due to reduction of resistance by sources.

In construction of four probe technique there are four metal tips [59]. Each tip has finite value of radius. Systematically diagram of this technique is shown in the figure. Amount of current is applied to two outer tips whereas voltage is applied to two inner tips to determine the value of resistivity. Ammeter and voltmeter also connected for measurement of current and voltage. The specific value between probe spacing is approximately equal to 1mm.

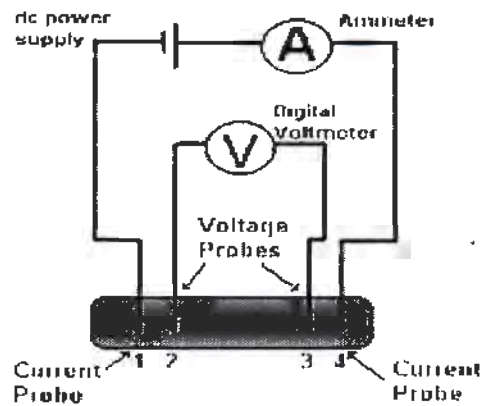


Fig.3.12: Four probe technique[60].

CHAPTER 4**Results and Discussion****4.1 XRD Analysis**

For crystal structure and phase purity X-ray diffraction (XRD) technique was used. XRD pattern for CuTi-1223 superconductor and 1.0 wt. % Cr nanoparticles included (Cr)_x/CuTi-1223 composites are shown in Fig. 4.1. It is shown from XRD that all major peaks are well indexed according to the tetragonal structure of P4/mmm symmetry and showed the dominance of CuTi-1223 phase. XRD pattern revealed that crystal structure of host CuTi-1223 phase was not affected after inclusion of Cr nanoparticles. Few un-indexed peaks of low intensities were also observed in XRD spectra, which showed the existence of impurities and other superconducting phases. Trademark diffraction peaks of CuTi-1223 superconductor recorded at $2\theta = 5.75$ in XRD pattern of (Cr)_x/CuTi-1223 nanoparticles-superconductor composites with $x = 0$ and 1.0 wt. %. There is no significant change observed in the overall XRD pattern of nano-Cr particles added (Cr)_x/CuTi-1223 samples, which gives a clear indication about the occupancy of these nanoparticles at the inter-crystallite sites of CuTi-1223 superconducting matrix. The presence of these nanoparticles at the grain boundaries can help to heal up the voids and to improve the weak-links [61-64].

Check Cell programming was used to ascertain cell parameters. Cell parameter of CuTi-1223 superconductor are found to be $a = 4.1\text{\AA}$ and $c = 15.18\text{\AA}$ and for 1.0 wt. % expansion of Cr nanoparticles in CuTi-1223 superconductor composites, cell parameters $a = 4.1\text{\AA}$ and $c = 15.20\text{\AA}$ were observed. The stoichiometry of CuTi-1223 matrix remains unaffected after inclusion of Cr nanoparticles; however a slight variation in the c-axis length is possibly due to stress and strains produced in the materials and the decrease of oxygen after addition of Cr-nanoparticles, which can change the apical bond length.

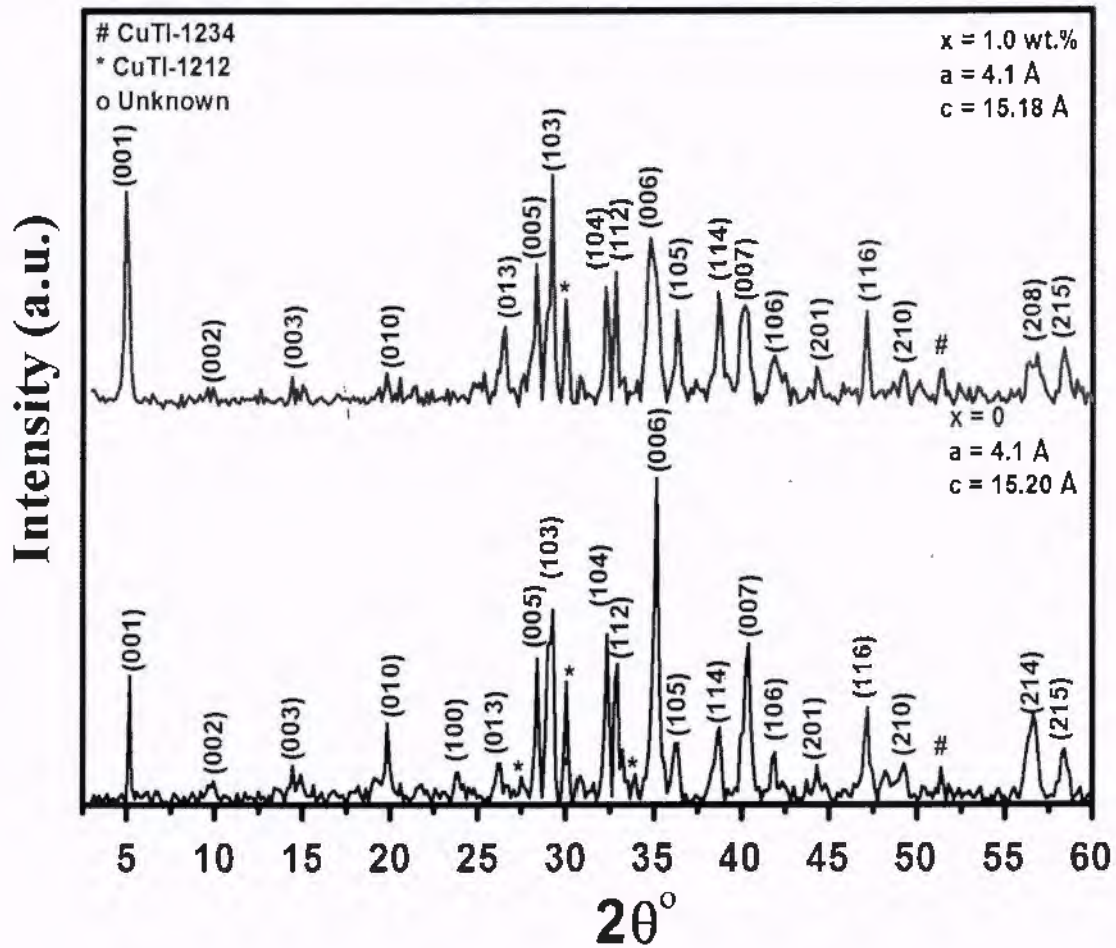


Fig.4.1: XRD of (Cr)_x/CuTi-1223 composites with (a) x = 0, (b) x = 1.0 wt. %.

4.2 Resistivity measurement

The dc-resistivity versus temperature (R-T) measurements of (Cr)_x/CuTi-1223 with x = 0, 0.25, 0.5, 0.75 and 1.0 wt. % are shown in Fig. 4.2 and in the inset is shown the variation of $T_{c(0)}$ (K) and normal state resistivity $\rho(\Omega\text{-m})$ versus Cr nanoparticles contents. These measurements show metallic variation from 260 K down to onset of superconductivity for all these samples. The value of $T_c(0)$ was found around 102, 100, 93, 92 and 90 K for x = 0, 0.25, 0.5, 0.75 and 1.0 wt. % respectively. The value of $T_{c(0)}$ (K) overall has been decreased with increasing Cr nanoparticles contents in CuTi-1223 superconducting matrix. As these nanoparticles creates oxygen vacancy disorder and ultimately reduced the carrier concentration in superconducting planes. These magnetic nature nanoparticles are settled at grain-boundaries

and enhance the scattering cross-section of carriers which result in Cooper pair breaking mechanism across grain-boundaries [65- 67]. The inclusion of Cr-nanoparticles suppresses the superconducting properties without affecting the structure of the host CuTi-1223 matrix. The normal state resistivity also increased due to inhomogeneous and non-uniform distribution of these nanoparticles across grain-boundaries.

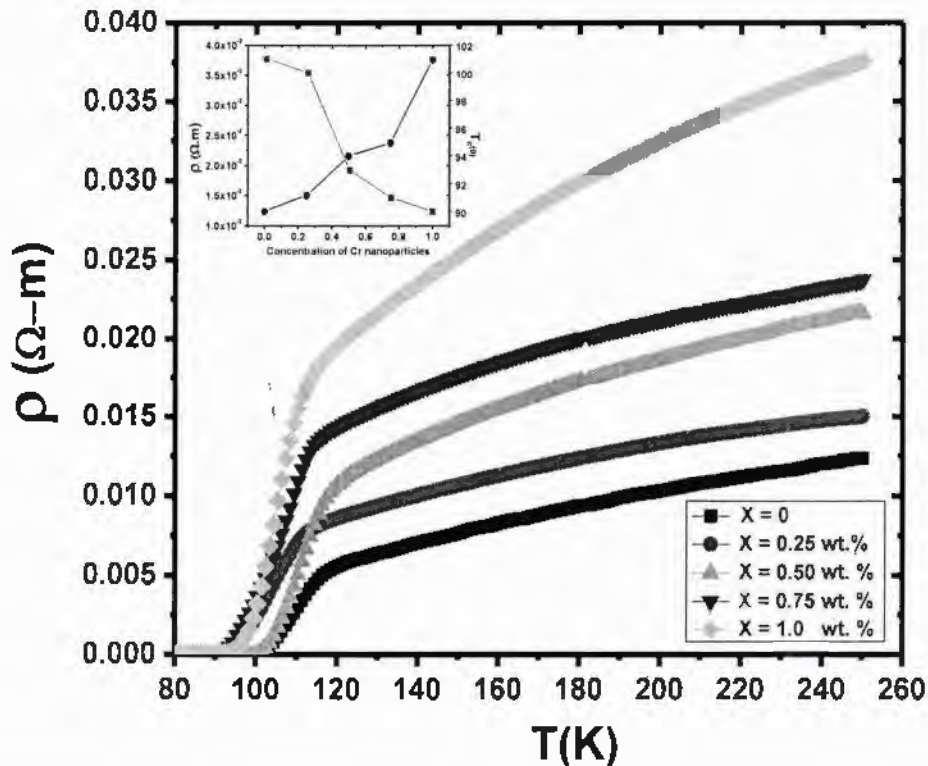


Fig.4.2: Resistivity vs temperature measurements of $(\text{Cr})_x/\text{CuTi-1223}$ nano-superconductor composite with $x = 0, 0.25, 0.5, 0.75$ and 1.0 wt. %.

4.3 Dielectric Properties

Tuning of dielectric properties of $(\text{Cr})_x/\text{CuTi-1223}$ ($x = 0, 0.25, 0.50, 0.75$ and 1 wt. %) as a function of frequency ranging from 40 Hz to 100 MHz at various temperature from 78 to 300 K were studied. Different properties of dielectric like real part, imaginary part and dielectric loss tangent have been studied. Dielectric properties of sample are found to be in good agreement with Maxwell-Wagner model and Koop theory. According to Koop's model grain is considered

as conducting layer and grain-boundaries are considered as resistive layers. So it is supposed that simple structure has two layers.

- Grain boundaries that behave as a poor conductor.
- Large grains that behave a good conducting layers.

4.3.1 Real part of dielectric constant (ϵ'_r)

When the sample is exposed to an electric field then some part of energy is stored within the material is given by real part of dielectric constant (ϵ'_r). Dielectric constant of the considerable number of tests are ascertained in the recurrence extend from 10 kHz to 10 MHz at various temperatures from 78 to 300 K. Variation of real part of (Cr)_x/CuTi-1223 nanoparticles-superconductor composites with $x = 0, 0.25, 0.50, 0.75$ and 1.00 wt.% as a function of frequency at various operating temperatures is shown in Fig. 4.3 (a-c).

Large increase in (ϵ'_r) at lower frequency for all samples correspond to Max -Well-Wegner effect, which is attributed to inhomogeneous dielectric structure. Space charge polarization is also another reason for the increase of real part at lower values of frequency. With the increase of frequency, ϵ'_r starts decreasing because the available time for drift of charge carriers is reduced [68-71]. Another reason for the decrease of ϵ'_r is the polarizibility associated with material rather than interfaces. As time constant of applied field is less than for time constant of dipolar polarization, so oscillations becomes fast, which gives rapid decrease in the values of ϵ'_r . At higher frequencies, ϵ'_r is constant, which indicates that external applied field cannot drift the charge carriers. In this region electronic and lattice polarization contribute due to very short relaxation time. In frequency range from 10^6 to 10^8 Hz hump has been observed in ' ϵ'_r ' versus 'f (Hz) curves, which is probably due to physical barrier that restrain charge migration. At this hump a maximum loss occurs. This hump is also called dielectric resonance and defined as when hooping frequency of electrons is equal to frequency of external applied electric field.

Dielectric behavior of ferrites and cuprates can be explained on the basis of Maxwell Wagner models and Koop theory. Koop model is considered as two layers model with grains and grain-boundaries. Grain is considered as conducting layer and grain-boundaries are considered as resistive layers. Electrons reach from conducting to non-conducting by hooping processes when

external field is applied. Dielectric constant decreases at higher frequencies due to lagging of electrons as they have difficulty to reach from grains to non-conducting regions. Maximum values of ϵ'_r at frequency of 40 Hz varied from 1.3×10^3 to 8.4×10^4 , 1.7×10^3 to 3.7×10^3 , 3.4×10^4 to 5.0×10^4 and 1.4×10^4 to 2.3×10^4 at 78 to 300 K for $x = 0, 0.25, 0.50, 0.75$ and 1.00 wt. % in $(\text{Cr})_x/\text{CuTi-1223}$ nanoparticles-superconductor composites.

In the insets of Fig. 4.3 (a-e), the variation of ϵ'_r versus operating temperature at low frequency of 40 Hz is shown. It was observed that by increasing temperatures from superconducting state to normal state, real part of ϵ'_r was increased for all samples which is probably due to increasing polarizability of the material. Over all non-monotonic trend shown after inclusion of Cr-nanoparticles for all samples which is most probably due to inhomogeneous distribution of these nano particles at grain boundaries of CuTi-1223 matrix

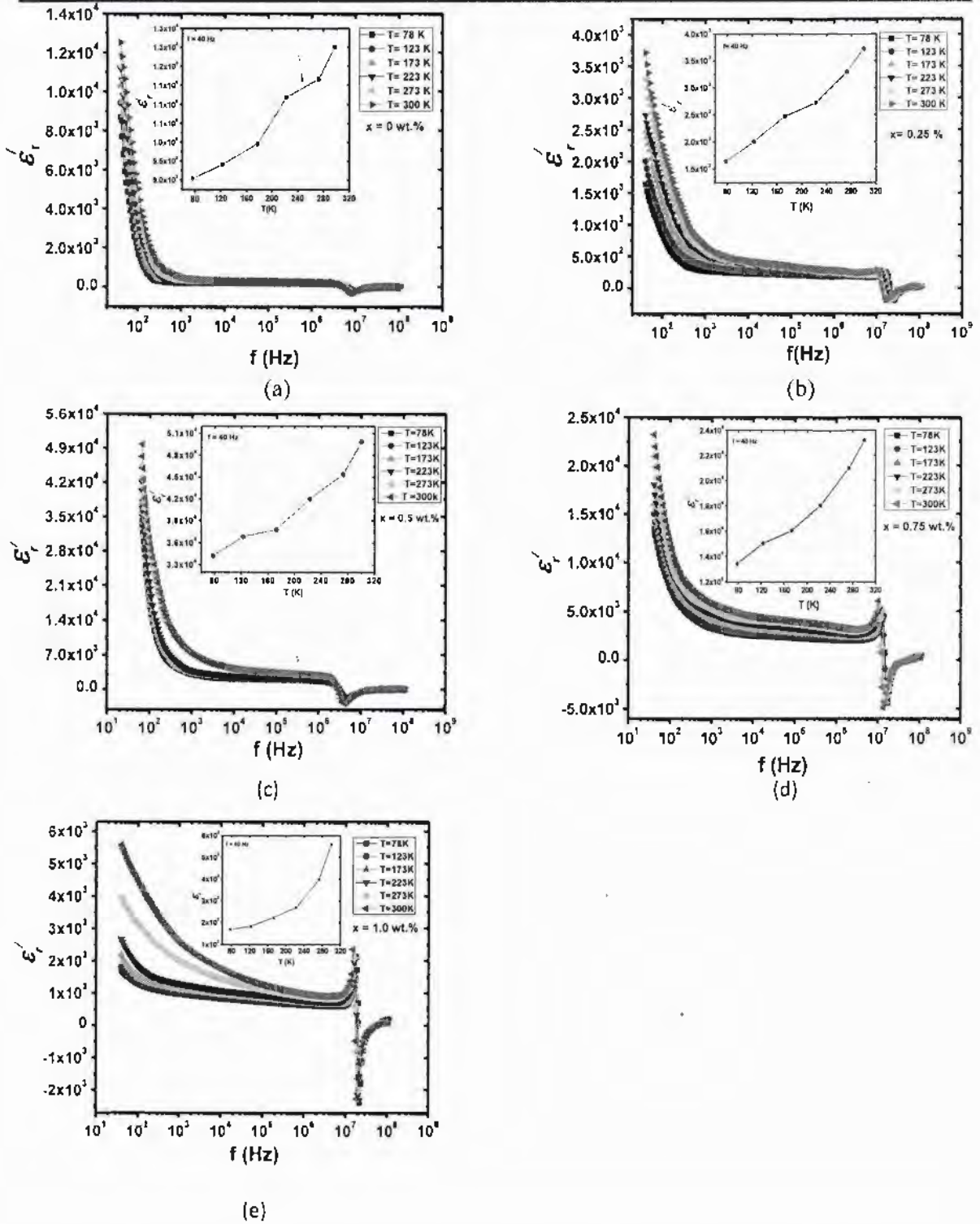


Fig.4.3 (a-e): Real part of dielectric constant of $(Cr)_x/CuTi-1223$ nano-superconductor composite samples with different concentrations of Cr nanoparticles (a) 0 (b) 0.25% (c) 0.50% (d) 0.75% (e) 1.0 wt.%. (f) Variation of real part of dielectric constant

4.3.2 Imaginary part of dielectric constant

The information regarding absorption of energy at interfaces is provided by imaginary part of the dielectric constant. Fig. 4.4 shows imaginary part of dielectric constant of $(\text{Cr})_x/\text{CuTi-1223}$ nanoparticles-superconductor composite samples with $x = 0, 0.25, 0.50, 0.75$ and 1.00 wt.% in the frequency range of 10 kHz to 10 MHz at different temperatures from 78 to 300 K .

Imaginary part of dielectric constant depends upon real part of dielectric constant and dielectric loss tangent. The reason for this behaviour of imaginary part of dielectric constant can be explained with the help of Maxwell-model and Koop's theory. According to this model the grain-boundaries are more active as compared to conducting grains at lower frequencies.

Highest value of imaginary part of dielectric constant varies from 3.3×10^7 to 3.9×10^7 , 6.0×10^4 to 4.3×10^5 , 1.2×10^8 to 1.7×10^8 , 7.48×10^7 to 9.9×10^7 and 7.3×10^6 to 9.5×10^6 in $(\text{Cr})_x/\text{CuTi-1223}$ nanoparticles-superconductor composites having concentrations of $x = 0, 0.25, 0.50, 0.75$ and 1.00 wt.% of Cr nanoparticles by varying temperature from 78 to 300 K . Insets in Fig. 4.4 (a-c) are showed the increasing trend of imaginary part of dielectric constant with increase in temperature. This increasing trend of imaginary part of dielectric constant is due to enhancement of polarization as a function of temperature in the material [72]. The non-monotonic variation in imaginary part of dielectric constant has been observed with increasing concentration of Cr nanoparticles. This non-monotonic variation is most probably due to non-uniform distribution of magnetic nature nanoparticles across grain-boundaries.

At lower frequencies imaginary part of dielectric constant found to be maximum which is most probably due to at lower frequency material easily respond to the electric field. At higher frequency imaginary part found to be zero because applied field cannot drift the charge carriers.

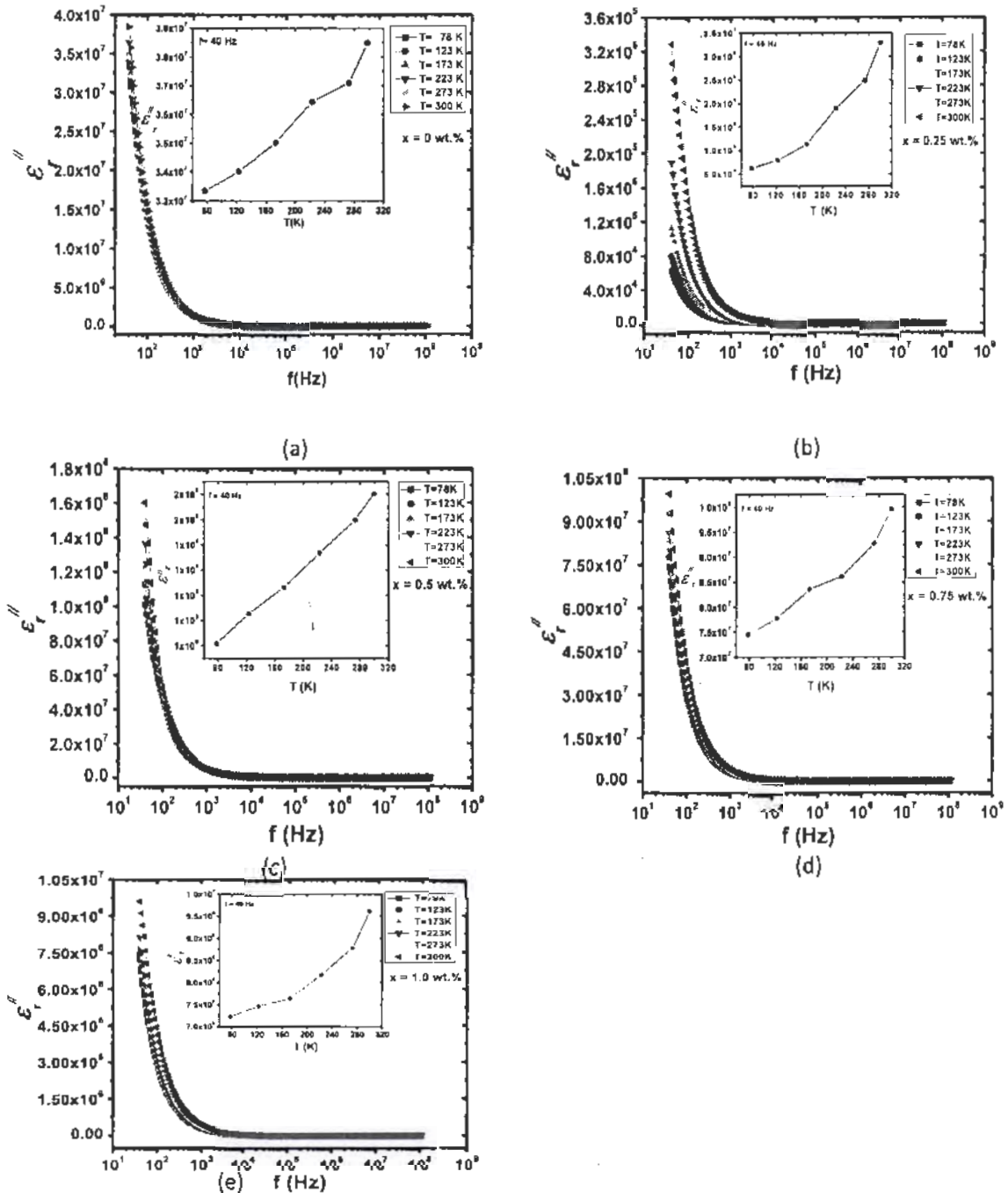


Fig. 4.4(a-e): Imaginary part of dielectric constant of $(Cr)_x/CuTl-1223$ nano-superconductor composite samples with different concentrations of Cr nanoparticles (a) 0 (b) 0.25% (c) 0.50% (d) 0.75% (e) 1.0wt.%. In the inset there shown a variation of imaginary part

4.3.3 Dielectric loss Tangent

Dielectric losses occur in dielectric materials is also known as dissipation factor denoted by 'D'. Dielectric loss tangent was determined with the help of LCR meter in the frequency range from 40 Hz to 100 MHz at different operating temperatures from 78-300K. Fig. 4.5 shows the dielectric loss tangent of $(Cr)_x/CuTi-1223$ composites with $x = 0, 0.25, 0.50, 0.75$ and 1.0 wt.%.

Dielectric loss tangent is the ratio between the imaginary and real parts of dielectric constant [73]. It depends upon synthesis technique, temperature of reaction and material structure. At low frequency region, dielectric loss tangent has been decreased with increase in frequency. Its value becomes maximum and then starts to decrease with further increase in frequency (i.e. at high frequency region) and showed a peak. Insets in Fig. 4.5 (a-e) showed decreasing trend of dielectric loss tangent with increase in temperature. This decreasing trend is due to release of space charges at grain-boundaries. Tangent loss depends upon different factors such as temperature, frequency, porosity, oxygen vacancies, and impurities. There is inverse relation between tangent loss and frequency for these materials. In polarization process, at lower frequencies grain-boundaries are more effective than conducting grains. Charges are piled up at grain-boundaries at lower frequency which gives high-value of dielectric loss tangent.

The value of 'tan δ ' is greater due to difficulties of hopping process of carriers and greater collisions with space charge carriers at lower frequencies. Hence, these charge carriers do not contribute in polarization. With increase in frequency, peaks of tangent loss (Tan δ) start decreasing and become saturated, which indicate that these charge carriers do not give response to applied electric ac-field.

The decrease in 'tan δ ' at higher frequencies occurs because the rate of hopping of charge carriers fails to follow the alternating electric field after a certain specific frequency and become almost constant. At certain frequencies the charge carriers do not follow the alternating applied field, which leads to decrease in dielectric permittivity and other dielectric parameters.

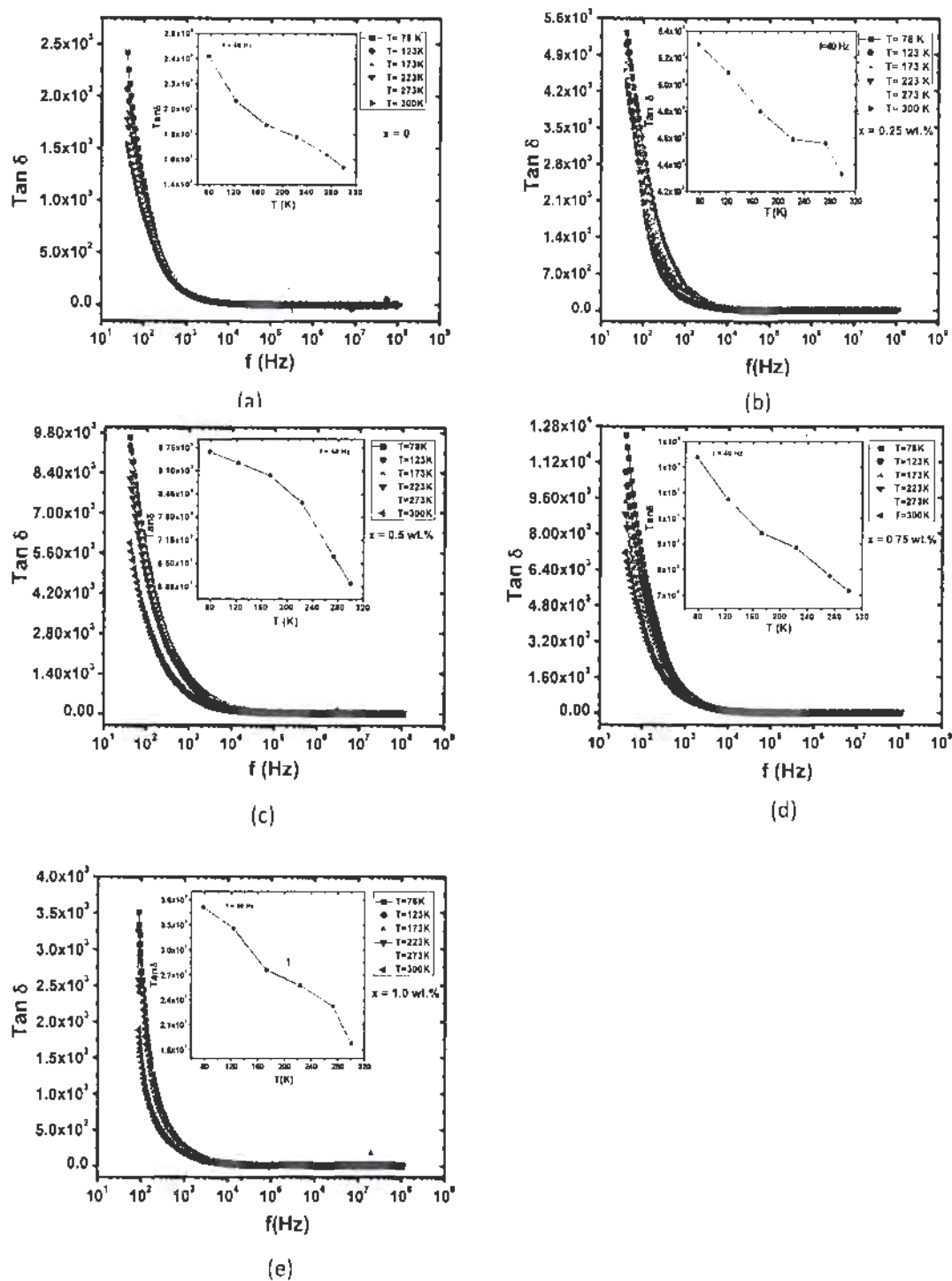


Fig.4.5 (a-e): Dielectric loss tangent of $(\text{Cr})_x/\text{CuTi-1223}$ nano-superconductor composite samples with different concentrations of Cr nanoparticles (a) 0 (b) 0.25% (c) 0.50% (d) 0.75% (e) 1.00 wt.%. In the inset there shown tangent loss vs temperature T .

Conclusion

Series of $(\text{Cr})_x/\text{CuTi-1223}$ ($x = 0, 0.25, 0.5, 0.75$ and 1.00 wt. %) nanoparticles-superconductor composites were synthesized successfully by sol-gel/solid state reaction method and characterized by different experimental techniques. Structural, superconducting and dielectric properties were explored by XRD, RT and LCR, respectively. Tetragonal crystal structure of CuTi-1223 matrix was not altered after the addition of Cr nanoparticles, which provides a clue about their occupancy at the grain-boundaries in the bulk CuTi-1223 material. The suppression of superconducting properties can be attributed due to the anti-ferromagnetic nature of Cr nanoparticles, which can minimize the mobility of the carriers. Dielectric parameters have decreased with the increase of frequency and became saturated at higher frequencies. Real part of dielectric constant showed a resonance peak at specific frequency while imaginary part and tangent loss of dielectric constant decreased with applied frequency. Real and imaginary part of dielectric constant increased while tangent loss decreased with applied operating temperature, which is due to the enhancement of polarizability in the material. Overall dielectric parameters show non-monotonic variation after inclusion of Cr nanoparticles which is due to inhomogeneous and non-uniform distribution of these nanoparticles at grain-boundaries.

References

References

- [1] Y. Wang, "Fundamental elements of applied superconductivity in electrical engineering", John Wiley and Sons, Singapore (2013).
- [2] Goodstein, and J. Goodstein, "Richard Feynman and the History of Superconductivity", *Phys. Perspect.* **2**, 30 (2000).
- [3] M. S. Vijaya, and G. Rangarajan, "Introduction to Material Science and Engineering", Tata McGraw-Hill publishing Company Limited, New Delhi (2004).
- [4] W. Pindt, and E. Schachinger, "Is a BCS-like theory sufficient to describe the superconducting state of Y-Ba-Cu-O?", *Physica B* **165**, 1091 (1990).
- [5] Z. Cheng, "Bose-Einstein condensation of interacting cooper pairs in cuprate superconductors", *Phys. Lett. A* **377**, 2007 (2013).
- [6] <http://hyperphysics.phy-astr.gsu.edu/hbase/Solids/meis.html>
- [7] O. B. Hyun, "Flux expulsion at intermediate fields in type-II superconductors", *Physica C* **206**, 169 (1993).
- [8] <https://en.wikipedia.org/wiki/Superconductivity>
- [9] H. Froehlich, "Theory of superconducting state", *Phys. Rev.* **79**, 845 (1950).
- [10] J. R. Schrieffer, "Handbook of high temperature superconductivity theory and experiment" Springer, New York (2007).
- [11] J. Seco, and T. A. Girad, "Nuclear Instruments and Methods in Physics Research Section A: Accelerators, Spectrometers, Detectors and Associated Equipment", Elsevier **444**, 360 (2000).
- [12] http://chemistry.pixel-online.org/EP_home01d4.html?id=03&tp=03
- [13] R. A. Klemm, and J. R. Clem, "Lower critical field of an anisotropic type-II superconductor", *Phys. Rev. B* **21**, 1868 (1980).
- [14] <https://www.slideshare.net/hardiksoni3o/superconductors-41816389>
- [15] A. V. Narlikar, "High temperature superconductivity", Springer, New York, (2004).
- [16] A. M. Hermann, and J. V. Yakhmi, "Thalium-Based High-temperature superconductors", 3th dition (1994).
- [17] A. Saleem, and S. T. Hussain, "Review the High Temperature Superconductor (HTSC) Cuprates-Properties and Applications", *J. Surf. Interf. Mater.* **1**, 23 (2013).

References

- [18] B. D. Jospheson, "Possible new effect in superconductive tunneling", *Phys. Lett.* **1**, 253 (1962).
- [19] S. O. Pillai, "Solid State Physics" 2nd Ed., New Age International New Delhi, (2009).
- [20] J. Bardeen, L. N. Cooper, and J. R. Schrieffer, "Theory of superconductivity" *Phys. Rev.* **108**, 1175 (1957).
- [21] https://commons.wikimedia.org/wiki/File:Cooper_pairs.jpg
- [22] S. Ramo, J. R. Whinnery, and T. V. Duzer, "Field and wave in communication electronics" 3rd Ed. **3**, 58551 (1994).
- [23] <http://hyperphysics.phy-astr.gsu.edu/hbase/electric/dietmllec.h>
- [24] <http://www.physicsclassroom.com/class/estatics/Lesson-1/Polarization>
- [25] <https://www.electrical4u.com/mechanism-of-polarization>
- [26] https://eng.libretexts.org/Core/Materials_Science/Properties/Dielectric_Polarization
- [27] S. Cavdar, H. Koralay, N. Tugluoglu, and A. Gunen, "Frequency-dependent dielectric characteristics of Tl-Ba-Ca-Cu-O bulk superconductor", *Supercond. Sci. Technol.* **18**, 1204 (2005).
- [28] L. F. Chen, C. K. Ong, C. P. Neo, V. V. Varadan, and V. K. Varadan, "Microwave Electronics" Wiley Blackwell (2004).
- [29] Toumey, and Chris, "Plenty of room, plenty of history", *Diss. Nature Publishing Group*,(2009).
- [30] <http://what-when-how.com/nanoscience-and-nanotechnology/nanocrystalline-materials-synthesis-and-properties-part-1-nanotechnology/>
- [31] N. T. Cherpak, and A. Y. Kirichenko, "Behaviour of quasi-optical dielectric resonators excited with high T_c superconductors in the temperature range 10–300 K", *Cryogenics* **31**, 387 (1991).
- [32] Y. Takahashi, H. Wakana, A. Ogawa, T. Morishita, and K. Tanabe, "Effects of La-doping on crystallinity and dielectric properties of $\text{SrAl}_0.5\text{Ta}_{0.5}\text{O}_3$ thin films for high- T_c superconductor multilayer structure", *Physica C* **392**, 1337 (2003).
- [33] C. Bernhardt, J. Humlicek, and B. Keimer, "Far-infrared ellipsometry using a synchrotron light source the dielectric response of the cuprate high T_c superconductors", *Thin Solid Films* **455**, 143 (2004).

References

- [34] S. Çavdar, H. Koralay, and S. Alhndal, "Effect of vanadium substitution on the dielectric properties of glass ceramic Bi-2212 superconductor" *J. Low Temp. Phys.* **164**, 102, (2011).
- [35] G. N. Pandey, K. B. Thapa, and S. P. Ojha, "Omni directional reflectance properties of superconductor-dielectric photonic crystal" *Optik* **125**, 252 (2014).
- [36] M. Mumtaz, M. Rahim, N. A. Khan, K. Nadeem, and K. Shehzad, "Dielectric properties of oxygen post-annealed $\text{Cu}_{0.5}\text{Tl}_{0.5}\text{Ba}_2\text{Ca}_3(\text{Cu}_{4-y}\text{Cd}_y)\text{O}_{12-8}$ bulk superconductor", *Ceram. Int.* **39**, 9591 (2013).
- [37] K. Yoshii, T. Fukuda, H. Akahama, J. Kano, T. Kambe and N. Ikeda, "Magnetic and dielectric study of Bi_2CuO_4 " *Physica C* **471**, 766 (2011).
- [38] T. Lia, J. Chena, D. Li, Z. Zhang, Z. Chen, Z. Li, X. Cao, and B. Wang, "Effect of NiO-doping on the micro structure and the dielectric properties of $\text{CaCu}_3\text{Ti}_4\text{O}_{12}$ ceramics", *Ceram. Int.* **40**, 9061 (2014).
- [39] A. Bisen , A. Satapathy , S. Parida , E. Sinha , S. K. Rout , and M. Kar, "Structural, optical band gap, microwave dielectric properties and dielectric resonant antenna studies of $\text{Ba}_{(1-x)}\text{La}_{(2x/3)}\text{ZrO}_3$ ($0 < X < 0.1$) ceramics", *J. Alloys Compds.* **615**, 1006 (2014).
- [40] K. Y. Tan , K. B. Tan, K. P. Lim , H. Jumiah , S. A. Halim , and S. K. Chen, "Frequency dependent dielectric properties of polycrystalline MgB_2 ", *Ceram. Int.* **42**, 10266 (2016).
- [41] M. Mumtaz, L. Ali, A. Jabbar, M. W. Rabbani, M. Naveed, M. Imran , B. Amin , M. N. Khan , and M. U. Sajid, "Tuning of dielectric properties of $(\text{ZnO})_x/(\text{CuTi-1223})$ nanoparticles-superconductor composites", *Ceram. Int.* **42**, 11193 (2016).
- [42] S. K. Hodak and C. T. Rogers, " Microstructure and dielectric response of $\text{SrTiO}_3/\text{NdGaO}_3$ interdigitated capacitors" *Microelectron. Eng.* **85**, 444 (2008).
- [43] B. Heeb, S. Oesch, P. Bohac, and L. J. Gauckler, "Microstructure of melt-processed $\text{Bi}_2\text{Sr}_2\text{CaCu}_2\text{O}_y$ and reaction mechanisms during post heat treatment", *J. Mater. Res.* **7**, 11 (1992).
- [44] C. N. Rao and R. Rao, "Chemical insights into High-Temperature Superconductors", *Phil. Trans. R. Soc. A* **336**, 595 (1991).
- [45] C. Giacovazzo, "Fundamentals of Crystallography", Oxf. Uni. Press, USA, (2002).
- [46] B. E. Warren, "X-ray Diffraction" Reading Mass. Addison-Wesley Pub. Co, (1969).
- [47] C. Giacovazzo, H. L. Monaco, G. Artiole, D. Viterbo, G. Ferraris, G. Gilli, G. Zanotti, and M. Catti, "Fundamentals of crystallography" , Oxf. Uni. Press, U .S. A, (2002).

References

- [48] <http://www.microscopy.ethz.ch/bragg.htm>.
- [49] J. Friedel, "Dislocations: International series of monographs on solid state physics" Pergamon Press Ltd. U. S. A (1964).
- [50] H. P. Klug, and L. E. Alexander, "X-Ray diffraction procedures for polycrystalline and amorphous materials" A Wiley-Interscience Publication Ist. Ed. (1954).
- [51] N. L. Wuet, "A method for preparation of the superconducting $Tl_2CaBa_2Cu_2O_8$ compound", Mater. Lett. **7**, 169 (1988).
- [52] B. B. He, U. Preckwinkel, and K. L. Smith, "Fundamentals of two-dimensional X-rays diffraction (XRD)" Adv. X-rays Anal. **43**, 273 (2000).
- [53] https://www.noao.cdu/image_gallery/text/fwhm.html.
- [54] S. Bertazzo, E. Gentleman, K. L. Cloyd, A. H. Chester, M. H. Yacoub, and M. M. Stevens, "Nano-analytical electron microscopy reveals fundamental insights into human cardiovascular tissue calcification" Nat. Mater. **12**, 576 (2013).
- [55] M. Joshi, and A. Bhatta, "Isothermal crystallization of HPDE/POSS nanocomposites", J. Appl. Poly. Sci. Willey Inter-Science **105**, 978 (2007).
- [56] M. Rajendran, R. C. Pullar, A. K. Bhattacharaya, and C. K. Majumdar, "Magnetic properties of nanocrystallite $CoFe_2O_4$ powder prepared at room temperature: variation with crystallite size", J. Magn. Mater. **232**, 71 (2001)
- [57] W. B. Weir, "Automatic measurement of complex dielectric constant and permeability at microwave frequencies", Proc. IEEE, **62**, 33(1974).
- [58] <http://www.bkprecision.com/products/component-testers/891-300khz-bench-lcr-meter.html>
- [59] N. Ashcroft, and N. Mermin, "Solid State Physics " Philadelphia, Pa. : Saunders college, (1976).
- [60] <http://www.imagesco.com/articles/superconductors/measuring-resistance-vs-temperature-and-critical-temperature.html>
- [61] I. Qasim, M. Waqee-ur-rehman, M. Mumtaz, G. Hussain, K. Nadeem, and N. A. Khan, "Role of anti-ferromagnetic Cr nanoparticles in $CuTl-1223$ superconducting matrix" J. Alloys Comp. **649**, 320 (2015).

References

- [62] S. Layek, and H.C. Verma. "Magnetic and dielectric properties of multiferroic BiFeO₃ nanoparticles synthesized by a novel citrate combustion method" *Adv. Mat. Lett.* **3**, 533 (2012).
- [63] J. Rout, R. Padhee, R. P. Das, and R. N.P. Choudhary. "Structural, dielectric and electrical properties of BiFeW₂O₉ ceramics" *Adv. Appl. Phys.* **1**, 105 (2013).
- [64] A. Jabbar, I. Qasim, K. M. Khan, Z. Ali, K. Nadeem, and M. Mumtaz "Synthesis and superconducting properties of (Au)_x/CuTl-1223 composites" *J. Alloys Compd.* **618**, 110 (2015).
- [65] G. Y. Hermiz, "Dielectric properties of Bi_{1.6}Pb_{0.4}Sr₂Ca_{2-x}Mg_xCu₃O_{10+δ} (0 ≤ x ≤ 0.5) superconducting system" *Int. j. innov. res. sci. eng. technol.* **3** 8564 (2014).
- [66] N. Novosel, and E. Babic, "Influence of magnetic nanoparticles on superconductivity of MgB₂" *Physica C* **493**, 119 (2013).
- [67] M. Mumtaz, and N. A. Khan, "Dielectric response of Cu_{0.5}Tl_{0.5}Ba₂(Ca_{2-y})(Cu_{0.5}Zn_{2.5})O_{10-δ} of bulk superconductor to frequency and temperature" *Physica C* **469**, 728 (2009).
- [68] R. K. Kotnala, V. Verma, V. Pandey, V. P. S. Awana, R. P. Aloysius, and P.C. Kothari, "The effect of nano-SiO₂ on the magnetic and dielectric properties of lithium cadmium ferrite", *Solid State Commun.* **143**, 527 (2007).
- [69] A. Younis, and N. A. Khan, "Dielectric properties of Cu_{0.5}Tl_{0.5}Ba₂Ca₃Cu_{4-y}Zn_yO_{12-δ} (y = 0, 3) superconductors" *J. Korean Phys. Soc.* **57**, 1437 (2010).
- [70] S. Suresh, "Synthesis, structural and dielectric properties of zinc sulfide nanoparticles" *Int. J. Phys. Sci.* **8**, 1121 (2013).
- [71] K. W. Wagner, "Dielectric properties of polycrystalline mixed nickel-zinc ferrites" *Anal. Phys.*, **40**, 817 (1913).
- [72] R. K. Nkum, M. O. Gyekye, and F. Boakye, "Normal-state dielectric and transport properties of In-doped Bi-Pb-Sr-Ca-Cu-O", *Solid State Commun.* **122**, 569 (2002).
- [73] X. Jiao, Z. Fu, M. Feng, L. Xu, K. Zuo and R. Chen, "Dielectric studies in a layered Ba based Bi-2222 cuprate Bi₂Ba₂Nd_{1.6}Ce_{0.4}Cu₂O_{10+δ}", *Physica C* **417**, 166 (2009).